

**JAERI-Data/Code
96-020**



**A POINT KERNEL SHIELDING CODE, PKN-HP,
FOR HIGH ENERGY PROTON INCIDENT**

June 1996

Hiroshi KOTEGAWA*

**日本原子力研究所
Japan Atomic Energy Research Institute**

本レポートは、日本原子力研究所が不定期に公刊している研究報告書です。

入手の問合せは、日本原子力研究所研究情報部研究情報課（〒319-11 茨城県那珂郡東海村）あて、お申し越しください。なお、このほかに財団法人原子力弘済会資料センター（〒319-11 茨城県那珂郡東海村日本原子力研究所内）で複写による実費頒布をおこなっております。

This report is issued irregularly.

Inquiries about availability of the reports should be addressed to Research Information Division, Department of Intellectual Resources, Japan Atomic Energy Research Institute, Tokai-mura, Naka-gun, Ibaraki-ken 319-11, Japan.

© Japan Atomic Energy Research Institute, 1996

編集兼発行 日本原子力研究所

印 刷 株原子力資料サービス

A Point Kernel Shielding Code, PKN-HP, for High Energy Proton Incident

Hiroshi KOTEGAWA*

Department of Reactor Engineering
Tokai Research Establishment
Japan Atomic Energy Research Institute
Tokai-mura, Naka-gun, Ibaraki-ken

(Received May 23, 1996)

A point kernel integral technique code PKN-HP, and the related thick target neutron yield data have been developed to calculate neutron and secondary gamma-ray dose equivalents in ordinary concrete and iron shields for fully stopping length C, Cu and U-238 target neutrons produced by 100 MeV-10 GeV proton incident in a 3-dimensional geometry. The comparisons among calculation results of the present code and other calculation techniques, and measured values showed the usefulness of the code.

Keywords: Proton Incident, Point Kernel Technique, Neutron, Secondary Gamma-ray, Dose Equivalent, HIL086R, Concrete, Iron, PKN-HP, Shielding Code, Neutron Yield Data

This report was prepared during his tenure of office.

* Retired from JAERI

高エネルギー陽子に対する点減衰核遮蔽計算コード：PKN-HP

日本原子力研究所東海研究所原子炉工学部

小手川 洋*

(1996年5月23日受理)

100MeVから10GeVまでの高エネルギー陽子入射による、陽子完全静止距離を有するC, Cu, U-238 標的中で発生する体積線源中性子に対して、普通コンクリート、鉄の遮蔽体を透過した中性子と2次 γ 線の線量当量を計算出来る点減衰核積分計算コードPKN-HP及びそのためのデータライブラリーを作成した。典型的な加速器施設の遮蔽体系についてのPKN-HPコードの計算結果を、他の簡易計算法による計算結果及び実験結果と比較することで、コードの有用性を検証した。

本報告書は著者が在職中に実施した研究の成果である。

東海研究所：〒319-11 茨城県那珂郡東海村白方白根2-4

*元原研職員

Contents

1. Introduction	1
2. Analytical Formulation of Point-kernel Code PKN-HP	2
2.1 Basic Formula	2
2.2 Thick Target Neutron Yield Data	3
2.3 Necessary Conditions for Application	4
3. Sample Calculations and Comparisons of the Results	5
4. Summary	8
Acknowledgments	8
References	9
Appendix	22

目 次

1. 序	1
2. 点減衰核積分法 PKN - HP の解析式	2
2.1 基本式	2
2.2 標的中性子利得データ	3
2.3 適用のための必要条件	4
3. 計算例と結果の比較	5
4. まとめ	8
謝 辞	8
参考文献	9
付 錄	22

1. Introduction

Recently, the present author et al. have calculated the attenuation data of neutron and secondary gamma-ray dose equivalents for point isotropic neutron sources up to 400 MeV in water, ordinary concrete and iron using ANISN-JR code¹⁾ and HILO86R cross section data^{2),3)} and expressed the calculated data with an exponential polynomial function, having 7 parameters. The parametrized data were installed in the point kernel integral technique code, PKN-H⁴⁾ which had been developed for application to neutron and secondary gamma-ray dose equivalent calculation in water, ordinary concrete and iron for 0.01 to 400 MeV neutron volume source.

In the present work, a point kernel integral technique code PKN-HP is developed based on PKN-H for shielding calculations of high energy proton beam incident by installing the thick target neutron yield data calculated with the Monte Carlo code system HERMES⁵⁾, and represented with an approximate formula. In PKN-HP code, the installed incident proton energy range is from 100 MeV to 10 GeV, target materials are C, Cu and U-238, and shield materials are ordinary concrete, iron and water. Moreover, the combinatorial geometry(CG) technique is used in the code to represent the target and shield geometries of 3-dimensional configuration. Geometrical routine of PKN-HP program is mainly based on that of QAD-P5A program⁶⁾ and the combinatorial geometry(CG) routine installed in PKN-HP is borrowed from MORSE-CG program⁷⁾.

In this report, the basic formula of PKN-HP and the characteristics of the installed target yield data are described, and the performance is discussed by comparing the results of the PKN-HP with other techniques for typical shielding problems. The input and output samples for the shielding problems are shown together with the input data instruction.

2. Analytical Formulation of Point-Kernel Code PKN-HP

2.1 Basic Formula

When high energy protons bombard a fully stopping-length target, secondary neutron production, due to incident proton-nucleus inelastic interaction, is dominant and secondary gamma-ray production, which follows after nucleon evaporation in the target, is very small in comparison with neutron production. The neutrons produced in the target attenuate producing the secondary gamma ray in the shield. Dose equivalent $H(E_p, r_R)$ due to the secondary neutrons and gamma-rays is calculated with the following equation,

$$H(E_p, r_R) = \int \int y_T(E_p, \Omega(r_p, r_n), E_n) \times H(E_n, r_S, r_R) dr_S dE_n , \quad (2.1)$$

where,

$$r_n \equiv r_R - r_S ,$$

r_p : incident proton coordinates,

r_R : coordinates of evaluation point,

r_S : coordinates of neutron source point within a target,

E_p : incident proton energy,

E_n : source neutron energy,

$H(E_n, r_S, r_R)$: dose equivalent for a neutron of energy E_n ,

$y_T(E_p, \Omega(r_p, r_n), E_n)$: double differential thick target neutron yield for incident proton of energy E_p (MeV) on a target T.

Thick target neutron yield y_T is represented approximately using the deformed moving source model, as follows,

$$y_T(E_p, \Omega(r_p, r_n), E_n) = \frac{A_1 \sqrt{E_n}}{(\pi \tau_1)^{3/2}} \exp(-E_n^*/\tau_1) + \frac{A_2 \sqrt{E_n}}{(\pi \tau_2)^{3/2} \sqrt{(E_n + \tau_1)}} \exp(-E_n^*/\tau_2) + \frac{A_3}{(\pi \tau_3)^{3/2} (E_n + \tau_2)} \exp(-E_n^*/\tau_3), \quad (2.2)$$

where definitions of E_n^* and θ are, as follows,

$$E_i^* = E_n + \varepsilon_i - 2\sqrt{E_n \varepsilon_i} \cos \theta, \quad (2.3)$$

θ : angle between the directions of incident proton and produced neutron in the laboratory frame.

And parameters, τ_i , ε_i and A_i are, as follows,

τ_i : Nuclear temperature parameter of each term($i=1,2,3$)(unit:MeV),

ε_i : Velocity parameter ($i=1,2,3$)(unit:MeV),

A_i : Amplitude of each term($i=1,2,3$),

(unit:n/p/MeV⁻¹/sr for $i=1$, n/p/MeV^{-3/2}/sr for $i=2$, n/p/MeV^{-5/2}/sr for $i=3$) .

The parameters, τ_i , ε_i and A_i for arbitrary proton energy between 10 MeV and 10 GeV are calculated automatically from a table installed in PKN-HP code using interpolation method. The first right hand term of y_T , eq.(2.2), expresses a contribution from evaporation neutrons which are postulated to have a Maxwell distribution. The second term describes a contribution from pre-equilibrium neutrons and the third term corresponds to cascade neutrons which are not postulated to have the Maxwell distribution, because of non-equilibrium state. The third term is truncated by an artificial condition of E_n , that is, $E_n < E_p \cos^4 \theta / 2$.

As seen from the above formula, parameters, τ_i , ε_i and A_i , have not exact physical meanings, and this point is different from the usual moving source models^{8,9,10)}. These parameters are used to reproduce the numerical results of thick target neutron yield calculated with HETC and MORSE codes equipped in HERMES code system⁵⁾ as precisely as possible in a wide proton energy range.

2.2 Thick Target Neutron Yield Data

The atom densities of target materials used are shown in Table 2.1. The length of thick target is chosen to stop fully the incident protons. Calculation conditions of thick target neutron yield with HETC down to 1 MeV neutron energy are given in Table 2.2. From that energy to 1 keV a coupling calculation using MORSE code equipped in HERMES code system is followed.

The double differential thick target neutron yield data calculated with HETC is compared with Meier et al.'s experiments for 113 MeV and 256 MeV proton incidents^{11,12,13)}, and relatively good agreements were obtained like as already mentioned in the literatures^{11,12,13)}. But, for 52 MeV proton incident the results of HETC calculation overestimated thick target neutron yield spectrum measured by Nakamura et al.¹⁴⁾. This can be attributed to the relatively rough model in HETC for the low

energy nuclear reaction. The reliable region of the thick target neutron yield data calculated with HERMES is, therefore, limited to the region from 100 MeV to several GeV proton incident.

2.3 Necessary Conditions for Application

Number densities of shield materials are shown in Table 2.3. Calculation conditions of attenuation data of dose equivalent in ordinary concrete, iron and water with ANISN-JR code, have been depicted in Appendix A.11.^{3,4)}

Energy group structure in target neutron yield calculation using the approximate formula eq.(2.2) is represented in Table 2.4. The number of neutrons of energy higher than 400 MeV produced in a target is stored in the first energy group(400-375 MeV). As for lateral shield which is placed parallel to proton incident direction, this approximation is not so influential for up to about 800 MeV proton incident, but above that energy and for forward shield configuration, some underestimation is predicted in the dose equivalent because of a little underestimation of attenuation length of dose equivalent for neutrons above 400 MeV.

Total thick target neutron yield is calculated with eq.(2.2) by integrating by E_n and θ , and the result reproduced values evaluated by Tesch¹⁵⁾ with relatively good accuracy for proton incident with energy above about 100 MeV, as seen in Appendix A.12. But, double differential thick target yield calculated with approximate formula eq.(2.2) shows sometimes 2-3 times overestimation at maximum in comparison with results calculated with HERMES except forward narrow angle(0° - 10°). The neutron yield calculated with the eq.(2.2) at forward narrow angle for above 500 MeV proton incident overestimates results calculated with HERMES one order higher at maximum in the neutron energy region below about 10 MeV because the eq.(2.2) can not represent forward neutron shielding effect due to large volume target. This fact is noticeable in a forward direction shielding calculation for high energy proton incident to fully stopping target, but not so serious because the overestimation to some extent may be permissible in the shielding design point of view.

3. Sample Calculations and Comparisons of the Results

Three kinds of typical sample calculations were made with the PKN-HP code, and the results were compared with those of other point kernel codes to verify the accuracy. The input manual for PKN-HP code is given in Appendix A.1.

Problem 1 : Dose equivalent calculation for a lateral 9 m thick concrete slab placed at 575 cm distant from a 10 cm length, 10 cm diameter cylindrical Cu target bombarded with 500 MeV protons (See Fig.3.1)

The input data of the Problem 1 is given in Appendix A.2 and output data is given in Appendix A.6.

As seen in Appendix A.13, which describes thick target neutron spectrum calculated with HETC for 500 MeV proton incident on Cu target, neutron yields over 400 MeV are negligible, and thus calculated results of PKN-HP for this problem has no special approximation about the thick target neutron yield spectrum. In Fig.3.2 comparisons of calculated results are shown. The result calculated with PKN-HP shows a very good agreement with result calculated with the Tesch's method¹⁵⁾ except of concrete surface region. The agreement is excellent especially at a region from 1 m to 7 m depth of concrete. Simplicity and usefulness of the Tesch's method are remarkable, however, its application is restricted to the lateral direction in the concrete shield. On the other hand, PKN-HP can be applied to calculations for arbitrary direction in the concrete, iron and water shields. Besides, secondary γ -ray dose equivalent in the shield can be estimated with the PKN-HP. Figure 3.2 also shows that the ratios of secondary γ -ray dose equivalent to neutron dose equivalent are 1/20 at around 1.2 m depth in the concrete shield and 1/30 to 1/40 at other points.

Problem 2 : Dose equivalent calculation for 1.5 GeV proton incident on U-238 rod target of 1.5 m length and 10 cm diameter placed at the center of semi-cylindrical air space, followed by 9 m thick concrete (See Fig.3.3)

The input and output data of the Problem 2 are given in Appendix A.3 and A.6, respectively.

Neutrons over 400 MeV produced by 1.5 GeV proton incident on U-238 target are stored in the first neutron energy group(400–375 MeV). This group structure may cause a little underestimation in the dose equivalent because the attenuation length of dose equivalent at neutron energy over 400 MeV is estimated a little lower.

As seen in Appendix A.14, however, the neutron yield in lateral direction(80° – 100° in the figure) over 400 MeV is very small, and it may be negligible. Calculated results are shown in Fig.3.4. As seen in the figure, there is a large discrepancy between results calculated with PKN-HP and Tesch's method¹⁵⁾.

Figure 3.5 shows dose equivalent distribution on a line 1 m deep in the concrete. The distributions have peak values at positions axially further than the source because it emits neutrons dominantly in the forward direction.

Problem 3 : Dose equivalent calculation at 0° , 22° , 45° and 90° directions for 230 MeV proton incident on cylindrical iron target of 7.51 cm length and 11.6 cm diameter placed at the center of a 1-m-diameter air sphere, followed by 4 m thick concrete having a density of 1.88 g/cm³ (See Fig.3.6)

The input and output data of the Problem 3 are given in Appendix A.4 and A.8, respectively. This sample problem is based on Siebers et al.'s experiments in 1990¹⁶⁾, where the density of the concrete shield is 1.88 g/cm³, while the density of concrete used in the PKN-HP is, however, 2.27 g/cm³.

Figure 3.7 shows the calculation results of PKN-HP comparing with Tesch's lateral results using concrete density $\rho = 2.27$ g/cm³. As seen in the figure, result of 90° direction calculated with PKN-HP shows a good agreement with result of Tesch's method except near inner surface region of the concrete spherical shell.

Figure 3.8 compares the PKN-HP results with, 1) those calculated with LAHET code system(shortly LCS¹⁷⁾) by Siebers et al.¹⁸⁾, 2) those calculated by Tesch's method using concrete density 1.88 g/cm³ and 3) those measured by Siebers et al.¹⁶⁾. Compared with measurements, the PKN-HP results show large overestimation, and at 0° and 22° , attenuation lengths of dose equivalents calculated with PKN-HP looks different from the measured one, at 45° and 90° , however, attenuation lengths of dose equivalents calculated with PKN-HP are very similar with

those of measurements, and following ratios of the two are observed,

$$\left| \begin{array}{c} H_{PKN-HP}(r) \\ \hline H_{exp}(r) \end{array} \right| \quad \approx 5.5 \text{ (for } 45^\circ \text{)}, \quad (3.1)$$

$50 \leq r \leq 300 \text{ (g/cm}^2\text{)}$

$$\left| \begin{array}{c} H_{PKN-HP}(r) \\ \hline H_{exp}(r) \end{array} \right| \quad \approx 5.5 \text{ (for } 90^\circ \text{)}. \quad (3.2)$$

$50 \leq r \leq 250 \text{ (g/cm}^2\text{)}$

In comparison with results calculated with LCS¹²⁾, the PKN-HP results show large overestimation, but seem to have a very similar attenuation length. And roughly speaking, the ratio of dose equivalent calculated with PKN-HP to that with LCS is found,

$$\left| \begin{array}{c} H_{PKN-HP}(r) \\ \hline H_{LCS}(r) \end{array} \right| \quad \approx 3.2, \text{ (for } 0^\circ, 22^\circ, 45^\circ, 90^\circ \text{)}, \quad (3.3)$$

$100 \leq r \leq 400 \text{ (g/cm}^2\text{)}$

for all angles.

In comparison with result calculated with Tesch's method, PKN-HP result shows large overestimation in the inner surface region, but beyond that region dose equivalent calculated with PKN-HP shows a satisfactory agreement with that of Tesch's method, as follows,

$$\left| \begin{array}{c} H_{PKN-HP}(r) \\ \hline H_{Tesch}(r) \end{array} \right| \quad \approx 1.3, \text{ (for } 90^\circ \text{)}. \quad (3.4)$$

$r \geq 350 \text{ (g/cm}^2\text{)}$

To be noted is results calculated with Agosteo et al.'s point kernel technique reported recently¹⁹⁾ which is characterized by classical two parameters, i.e., dose equivalent source term and its attenuation length, calculated with newly developed versions of hadron cascade Monte Carlo code, LCS¹⁷⁾ and FLUKA²⁰⁾. As seen in Fig.3.8, the results calculated with Agosteo et al.'s parameters reproduce measured values fairly well.

The dose equivalents calculated with Tesch's method and Agosteo et al.'s point kernel technique, however, can not represent the rapidly decreasing behavior of dose equivalent in the inner surface region of concrete, which is observed in the experimental results at 90° direction and PKN-

HP results.

4. Summary

A point kernel integral calculation code PKN-HP has been developed. This code can be applied to calculations of the neutron and secondary gamma-ray dose equivalents within and behind concrete, iron and water shields for C, Cu and U-238 targets bombarded with high energy protons in 3-dimensional geometry. The accuracy of the PKN-HP code has been verified by comparing the results with the calculation of Tesch's point kernel method and Monte Carlo codes, and also with the experimental results by Siebers et al..

Acknowledgments

The author wish to thank Dr. H. Yasuda for his continuous encouragements and valuable suggestions to this work. The author would like to appreciate the kind supports and useful advises by all specialists of Applied Radiation Laboratory of JAERI.

HP results.

4. Summary

A point kernel integral calculation code PKN-HP has been developed. This code can be applied to calculations of the neutron and secondary gamma-ray dose equivalents within and behind concrete, iron and water shields for C, Cu and U-238 targets bombarded with high energy protons in 3-dimensional geometry. The accuracy of the PKN-HP code has been verified by comparing the results with the calculation of Tesch's point kernel method and Monte Carlo codes, and also with the experimental results by Siebers et al..

Acknowledgments

The author wish to thank Dr. H. Yasuda for his continuous encouragements and valuable suggestions to this work. The author would like to appreciate the kind supports and useful advises by all specialists of Applied Radiation Laboratory of JAERI.

HP results.

4. Summary

A point kernel integral calculation code PKN-HP has been developed. This code can be applied to calculations of the neutron and secondary gamma-ray dose equivalents within and behind concrete, iron and water shields for C, Cu and U-238 targets bombarded with high energy protons in 3-dimensional geometry. The accuracy of the PKN-HP code has been verified by comparing the results with the calculation of Tesch's point kernel method and Monte Carlo codes, and also with the experimental results by Siebers et al..

Acknowledgments

The author wish to thank Dr. H. Yasuda for his continuous encouragements and valuable suggestions to this work. The author would like to appreciate the kind supports and useful advises by all specialists of Applied Radiation Laboratory of JAERI.

References

- (1) Koyama K. et al.: "ANISN-JR:A One-Dimensional Discrete Ordinates Code for Neutron and Gamma-Ray Transport Calculation", JAERI-M 6954(1977).
- (2) Kotegawa H. et al.: "Neutron-Photon Multigroup Cross Sections For Neutron Energies up to 400 MeV:HILO86R -Revision of HILO86 Library-", JAERI-M 93-020(1993). ORNL-RSIC Computer Code Collection, DLC-187/HILO86R(1996).
- (3) Kotegawa H. et al.: "Attenuation Data of Point Isotropic Neutron Sources up to 400 MeV in Water, Ordinary Concrete and Iron", JAERI-Data/Code 94-003(1994).
- (4) Kotegawa H. et al.: "PKN-H:A Point Kernel Shielding Code for Neutron Source up to 400 MeV", JAERI-Data/Code 95-004(1995).
- (5) Cloth P. et al.: "HERMES:A Monte Carlo Program System for Beam-Materials Interaction Studies", Jul-2203(1988).
- (6) Solomito E. and Stockton J.: "Modification of the Point-Kernel Code QAD-P5A:Conversion to the IBM-360 Computer and Incorporation of Additional Geometry Routines", ORNL- H -181 (1968).
- (7) ORNL-RSIC Computer Code Collection, CCC-203/MORSE-CG(1985).
- (8) Ishibashi K. et al.: "Moving Source Model Analysis of Neutron Production Cross Section for Proton Induced Spallation Reactions", Journal of Nucl. Sci. & Tech. 29, 499(1992).
- (9) Shin K. et al.: "Thick-Target Neutron Yield for Charged Particles", Nucl. Sci. Eng. 120, 40 (1995).
- (10) Shin K. et al.: "Systematics in Differential Thick-Target Neutron Yields Parametrized by Moving Source Model", Nucl. Sci. Eng. 120, 136(1995).
- (11) Meier M.M. et al.: "Differential Neutron Production Cross Sections and Neutron Yields from Stopping-Length Targets for 113-MeV Protons", Nucl. Sci. Eng. 102, 310(1989).
- (12) Meier M.M. et al.: "Neutron Yields from Stopping- and Near Stopping-Length Targets For 256 MeV Protons", Nucl. Sci. Eng. 104, 339(1990).
- (13) Meier M.M. et al.: "Neutron Yields from Stopping-Length Targets For 256-MeV Protons", Nucl. Sci. Eng. 110, 299(1992).
- (14) Nakamura T. et al.: "Neutron Production from Thick Targets by Protons in the Energy Range 30 to 50 MeV", Nucl. Sci. Eng. 83, 444(1983).
- (15) Tesch K.: "A Simple Estimation of the Lateral Shielding for Proton Accelerators in the Energy Range 50 to 1000 MeV", Radi. Prot. Dosim. 11, 165(1985).
- (16) Siebers J.V. et al.: "Shielding Measurements for 230-MeV Protons", Nucl. Sci. Eng. 115, 13(1993).

- (17) Prahl R.E. and Lichtenstein H.: "Users Guide to LCS : The LAHET Code System", LA-UR-89-3014, Los Alamos National Laboratory(1989).
- (18) Siebers J.V., et al.: "Shielding Calculations for 230 MeV Protons Using the LAHET Code System", Nucl. Sci. Eng. 122, 258(1996).
- (19) Agosteo S., Fasso A., Ferrari A., Sala P.R., Silari M. and Tabanelhi de Fatis P.: "Double Differential Distribution and Attenuation in Concrete for Neutrons Produced by 100-400 MeV Protons on Iron and Tissue Targets", Nucl. Instru. Methods, to be published(1996).
- (20) Fasso, A., Ferrari, A., Ranft, J., and Sala, P.R., Proc. of the AEN/NEA Specialists' Meeting on Shielding Aspects of Accelerators, Targets and Irradiation Facilities, Arlington(Texas), 28-29 April 1994, NEA/OECD, p.287(1995).

Table 2.1 Atom density of targets.

unit($10^{24}/\text{cm}^3$)

Material	C	Cu	U-238
Density	0.0852	Cu-63: 0.05874 Cu-65: 0.02618	0.0483

Table 2.2 Calculation conditions of HETC for thick target neutron yield data installed in PKN-HP code.

Code	HETC ^{S)} : Monte Carlo High-Energy Nucleon-Meson Transport Code
Model	Intranuclear-cascade and evaporation
Incident particle	20 MeV to 10 GeV energy protons
Target	Material : C, Cu and U-238 Size : Full stopping length
Detector	Track length detector
Geometry	3-dimensional cylinder
Calculation	Double differential thick target neutron yield from incident proton energy down to 1 MeV

Table 2.3 Atom density of shields.

unit($10^{24}/\text{cm}^3$)

	Ordinary Concrete	Iron	Water
H	1.3851-2		6.6738-2
C	1.1542-4		
O	4.5921-2		3.3369-2
Mg	1.2388-4		
Al	1.7409-3		
Si	1.6621-2		
K	4.6205-4		
Ca	1.5025-3		
Fe	3.4510-4	8.4869-2	
Density (g/cm^3)	2.27	7.87	1.00

Table 2.4 Energy group structure of target neutron

Group No.	Energy Range (MeV)	Group No.	Energy Range (MeV)
1	400-375	29	22.5-19.6
2	375-350	30	19.6-17.5
3	350-325	31	17.5-14.9
4	325-300	32	14.9-13.5
5	300-275	33	13.5-12.2
6	275-250	34	12.2-10.0
7	250-225	35	10.0-8.19
8	225-200	36	8.19-6.70
9	200-180	37	6.70-5.49
10	180-160	38	5.49-4.49
11	160-140	39	4.49-3.68
12	140-120	40	3.68-3.01
13	120-110	41	3.01-2.46
14	110-100	42	2.46-2.02
15	100-90	43	2.02-1.65
16	90-80	44	1.65-1.35
17	80-70	45	1.35-1.11
18	70-65	46	1.11-0.907
19	65-60	47	0.907-0.743
20	60-55	48	0.743-0.498
21	55-50	49	0.498-0.334
22	50-45	50	0.334-0.224
23	45-40	51	0.224-0.150
24	40-35	52	0.150-0.0865
25	35-30	53	0.0865-0.0318
26	30-27.5	54	0.0318-0.0150
27	27.5-25	55	0.0150-0.0071
28	25-22.5		

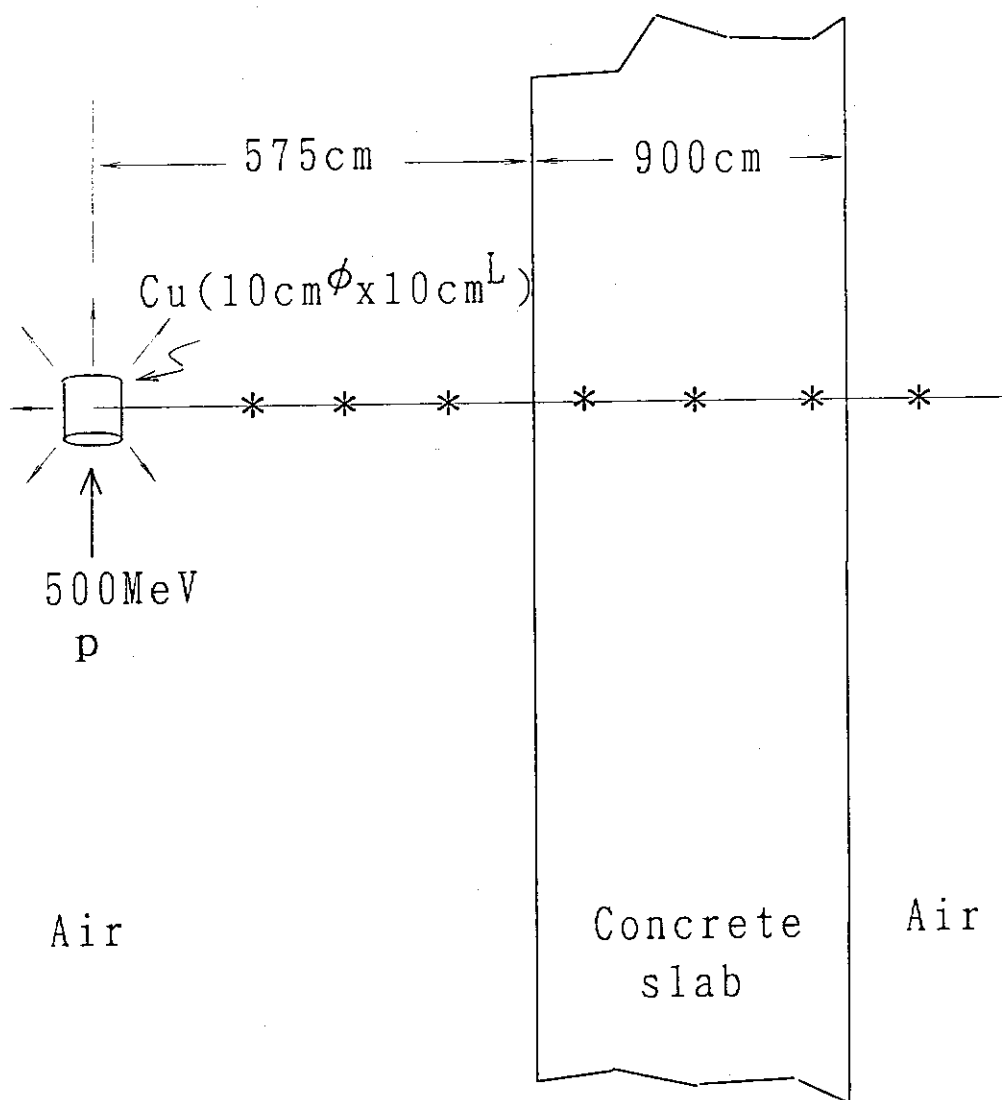


Fig.3.1 Calculational model of Problem 1

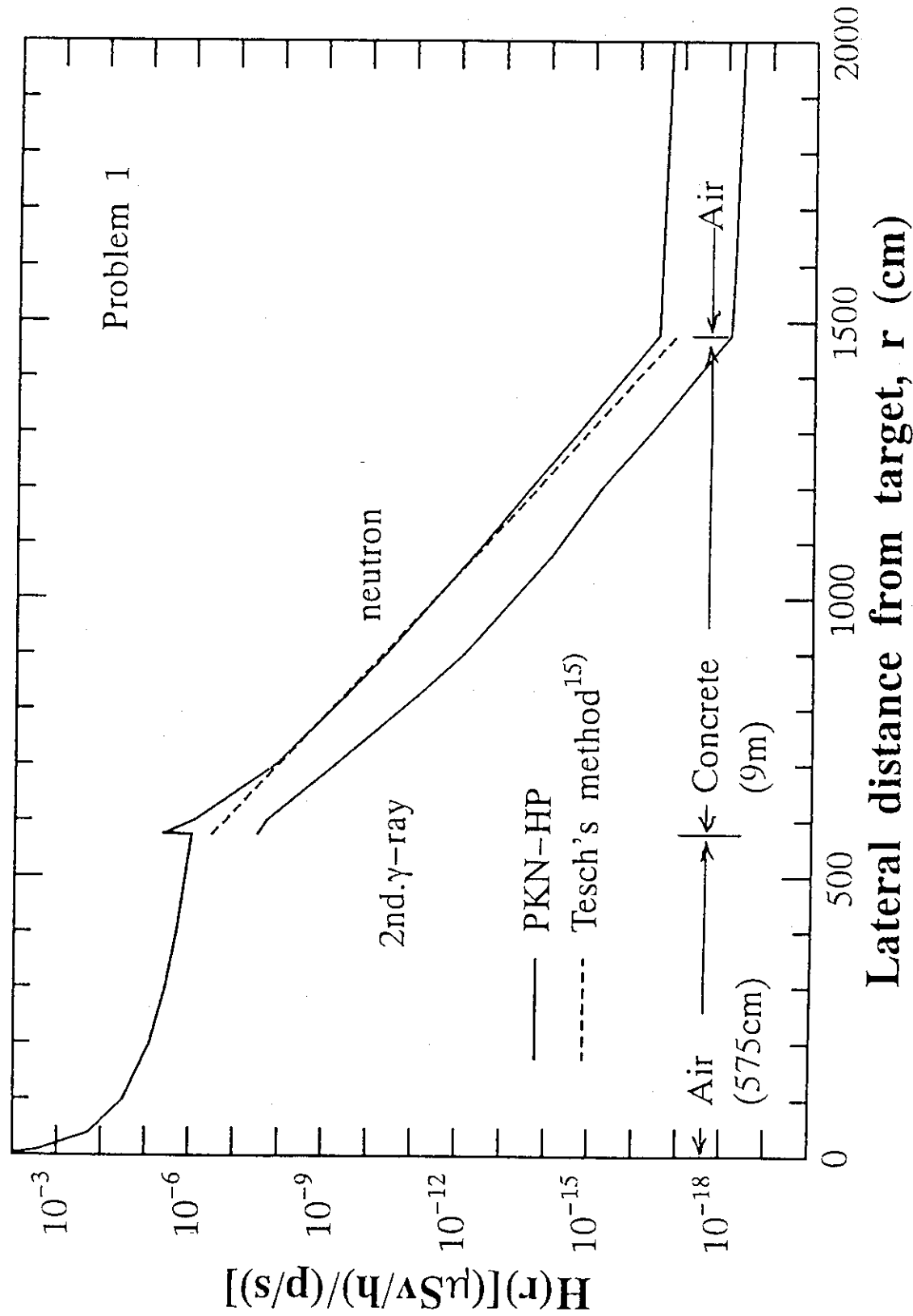


Fig.3.2 Calculation results of neutron and secondary gamma ray dose equivalents for Problem 1

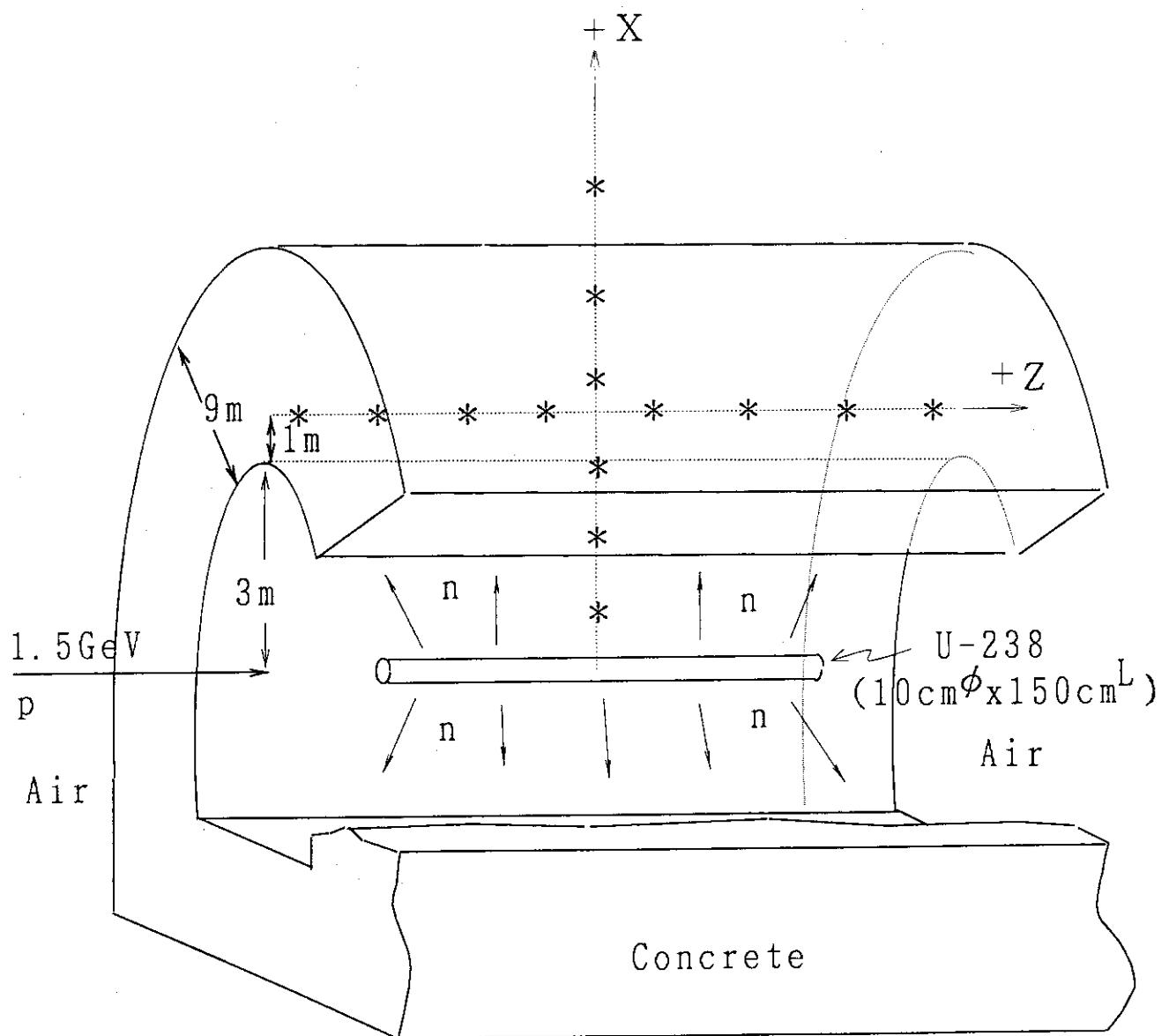


Fig.3.3 Calculational model of Problem 2

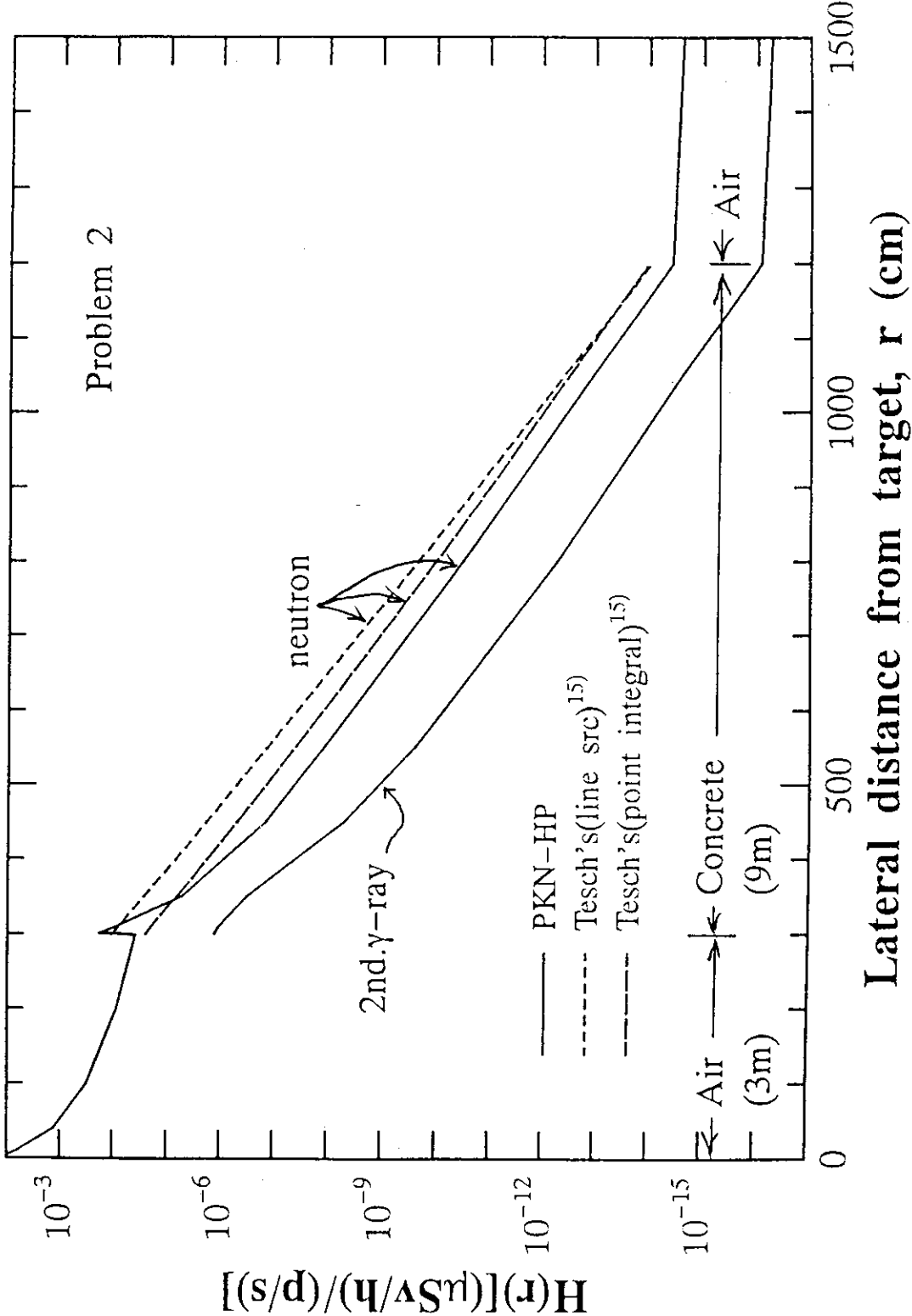


Fig.3.4 Calculation results of neutron and secondary gamma ray dose equivalent distribution in the direction perpendicular to line source for Problem 2

Calculated result of Tesch's method for line source is described by short dash line, while long dash line depicts a integrated value of neutron dose equivalent for point neutron source of Tesch's method along line source.

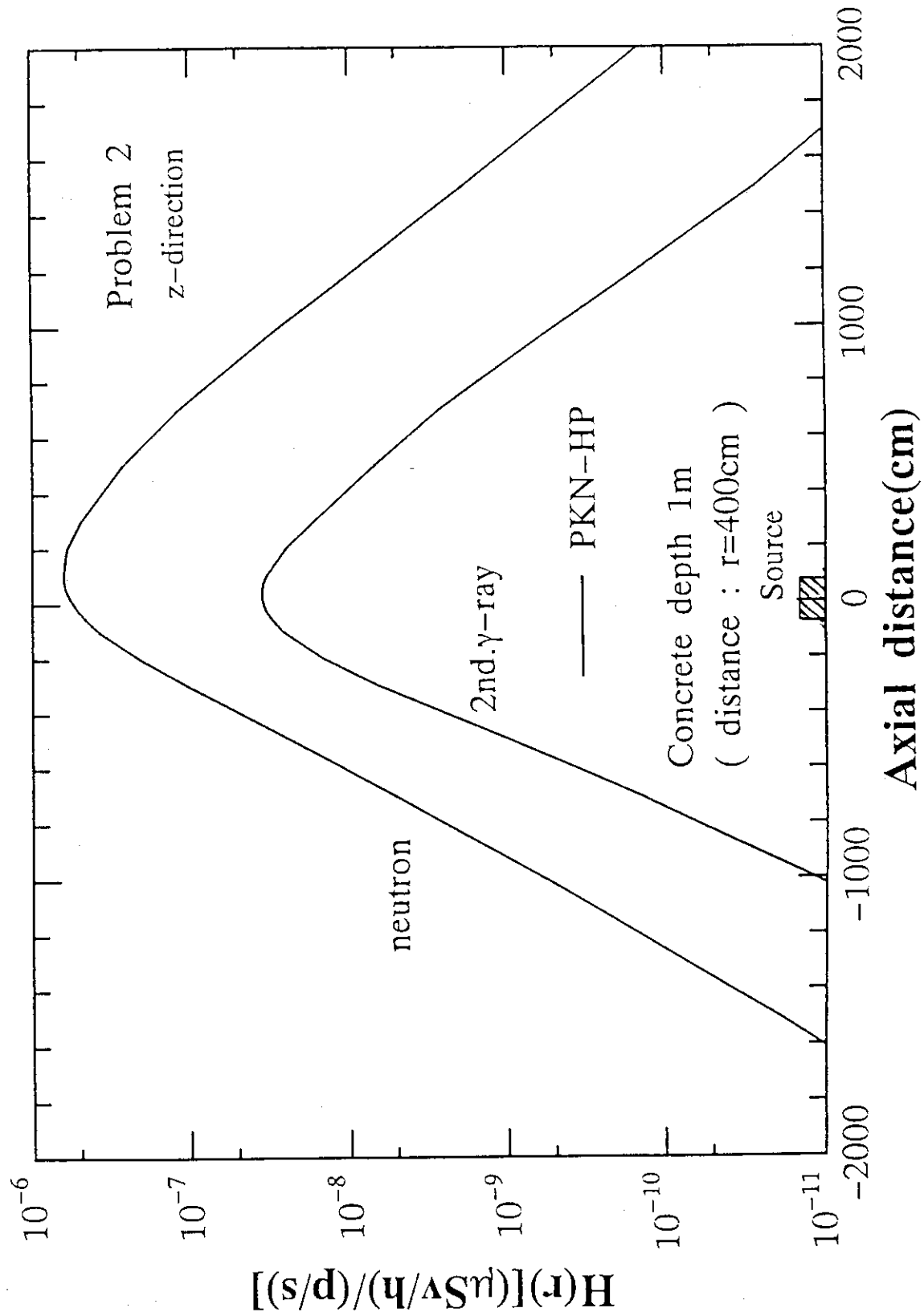


Fig.3.5 Calculation results of neutron and secondary gamma ray dose equivalent distribution in the direction parallel to line source for Problem 2

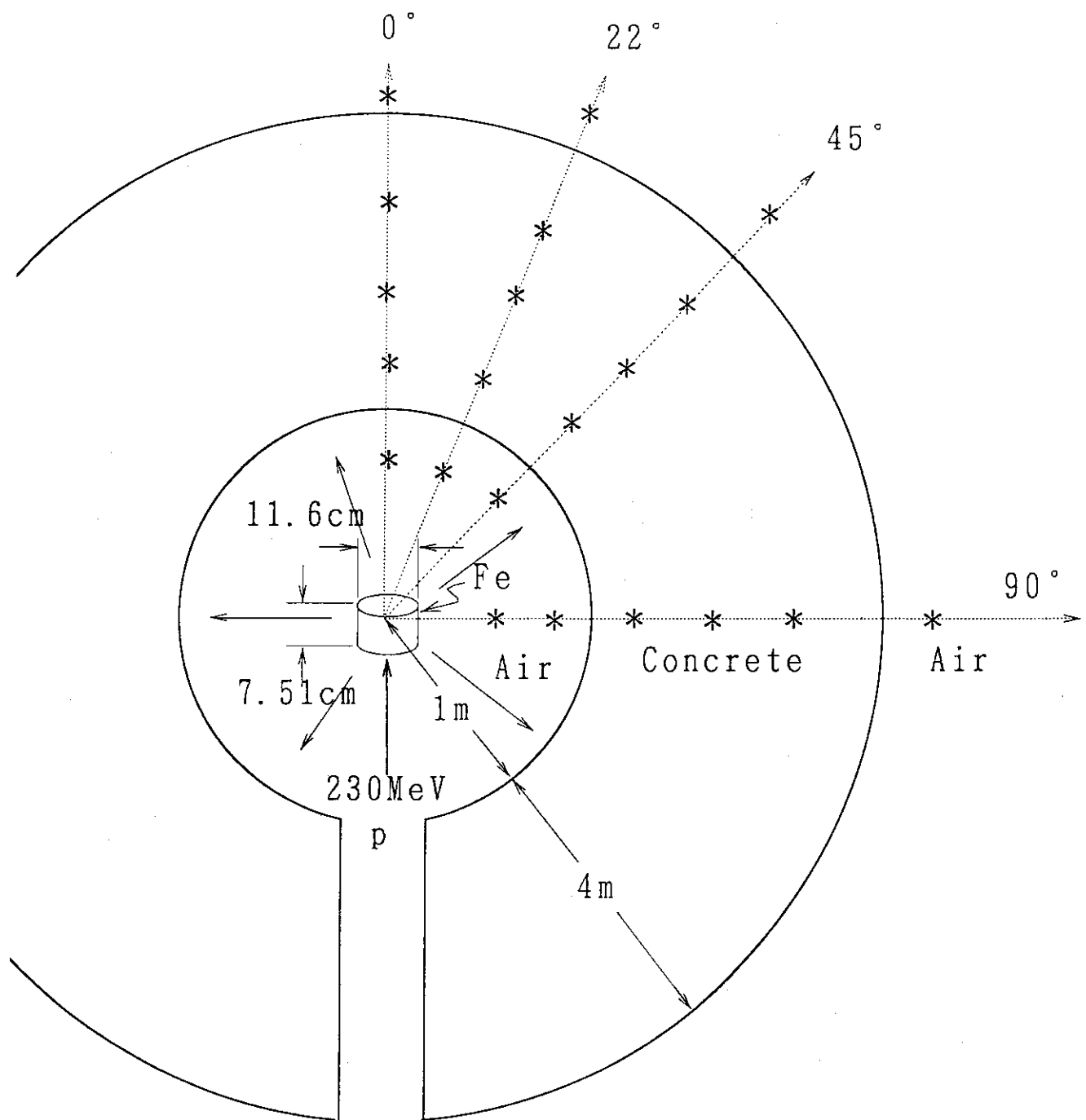


Fig.3.6 Calculational model of Problem 3

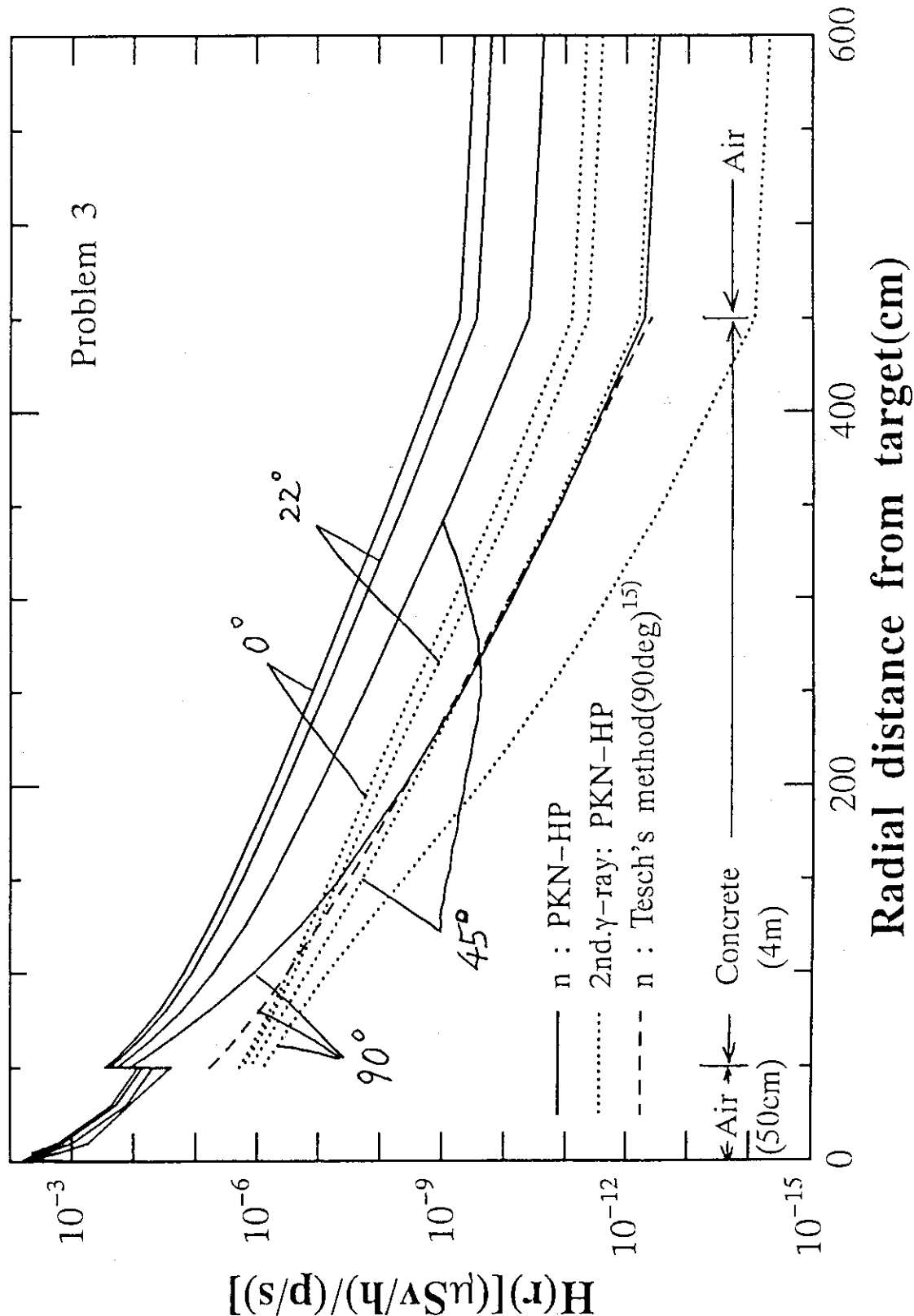


Fig.3.7 Calculation results of neutron and secondary gamma ray dose equivalents for Problem 3

Concrete density is 2.27 g/cm³ in both PKN-HP and Tesch's method calculations.

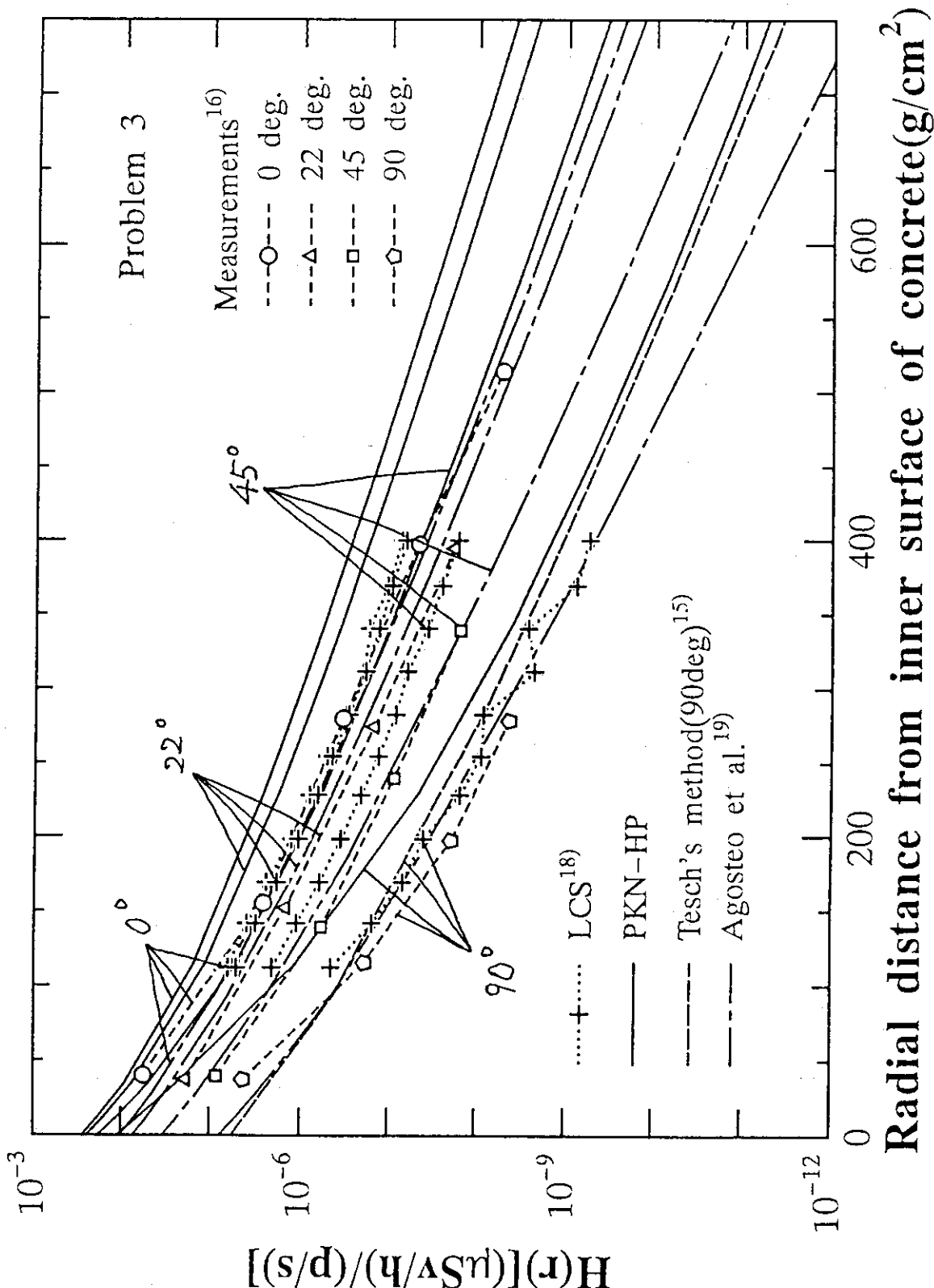


Fig.3.8 Comparison of calculated results of neutron dose equivalent with that of measurements for Problem 3
Concrete density is $1.88 \text{ g}/\text{cm}^3$ in all calculations except $2.27 \text{ g}/\text{cm}^3$ in PKN-HP calculation.

Appendix

A.1 Input manual of PKN-HP	23
A.2 Input data of the Problem 1	27
A.3 Input data of the Problem 2	29
A.4 Input data of the Problem 3	
A.5 Output of PKN-HP	31
A.6 Output data of the Problem 1	31
A.7 Output data of the Problem 2	32
A.8 Output data of the Problem 3	34
A.9 Input required on CGB cards for each body type	36
A.10 Description of body types	37
A.11 Calculation conditions of neutron and secondary gamma-ray dose equivalent attenuation data installed in PKN-HP	42
A.12 Comparisons of total thick target neutron yields between various target materials and between two evaluation methods	43
A.13 Double differential thick target neutron yield calculated with HETC for 500 MeV proton bombardment on full stopping length Cu target	44
A.14 Double differential thick target neutron yield calculated with HETC for 2 GeV proton bombardment on full stopping length U-238 target	45

Appendix A.1 Input manual of PKN-HP

It is necessary to prepare CARD P-A to CARD Z. The cartesian, spherical or cylindrical geometries are available, each 3-dimensional coordinates are expressed, generally, X1, X2 and X3. There axeses correspond X, Z and Y in the cartesian coordinates, R, Θ and Ψ in the spherical coordinates, and R, Z, and Θ in the cylindrical coordinates, respectively. Length and angle are to be inputed in unit of cm and degree, respectively.

CARD P-A to CARD P-D indicate incident proton information.

CARD P-A(A72);Title

CARD P-B(2E9.2);EPI,PNUM

EPI :Incident proton energy[MeV]

PNUM :Beam loss or normalization constant[1]

CARD P-C(E9.2);TGMS

TGMS :Target mass[1],(C/Cu/U-238)=(12/64/238)

CARD P-D(3F6.3);uuu,vvv,www

uuu,vvv,www;Incident proton direction unit vector indicate each x, y and z component

Note : When TGMS is selected to be an other number than 12, 64 or 238, interpolation of thick target neutron data parameters is performed, in which accuracy of calculated result may be less than the case of TGMS is 12, 64 or 238.

CARD A to CARD Z indicate shield configuration and location of receiver information.

CARD A(A72);Title

CARD B(14I4);

NSX1 : total number of input location of X1 coordinate of source

NSX2 : total number of input location of X2 coordinate of source

NSX3 : total number of input location of X3 coordinate of source

NREG : total number of regions (or zones) defined in CARD-CGC

NBOD : total number of bodies defined in CARD-CGB

NSOPT : coordinates system described the form of source

(0/1/2)=(Cylindrical/Cartesian/Spherical coordinates)

ISRC : Type of source

(0/1/2)=(source of the previous case is used/cosine-distributed source is used/source is

computed using the weighting values input along each coordinate axis)

CARD-C(E10.3,6I5);CID00((CID(I,J),I=1,2),J=1,3)

CID00 : The total source strength in fissions/sec, Captures/sec, or dacays/sec.(Default = 1)

CID : Constants for cosine source distribution.

(CID is ignored, if ISRC does not equal to 1.)

If ISRC equals 1, source strength distribution is calculated as following equation,

$$\text{Source strength}(X_1, X_2, X_3) = \text{CID00} * \cos(\text{CID}(1,1)*(X_1 - \text{CID}(2,1))$$

$$* \cos(\text{CID}(1,2)*(X_2 - \text{CID}(2,2)))$$

$$* \cos(\text{CID}(1,3)*(X_3 - \text{CID}(2,3))).$$

CARD-D(8E9.2);(SOX1(I),I=1,NSX1+1)

SOX1 : coordinates of source volume divisions along X1-axis.

CARD-E(8E9.2);(SOX2(I),I=1,NSX2+1)

SOX2 : coordinates of source volume divisions along X2-axis.

CARD-F(8E9.2);(SOX3(I),I=1,NSX3+1)

SOX3 : coordinates of source volume divisions along X3-axis.

Note: Source intensity is normalized to 1.

CARD-G(3E9.2,I9,E9.2);TSX1(I),TSX2(I),TSX3(I),ITS(I),WTS(I)

TEX1 : Center coordinate of I-th source volume along X1-axis.

TEX2 : Center coordinate of I-th source volume along X2-axis.

TEX3 : Center coordinate of I-th source volume along X3-axis.

ITS : Coordinate system describing center coordinates

(0/1/2)=(Cylindrical?Cartesian/Spherical coordinates)

WTS : Weight(ratio) of I-th source volume

Note: CARD-G iterates numbers of source blocks, if source separates into more than two blocks.

Note: I-th source coordinates is calculated, as follows,

$$(SOX1+TSX1(I),SOX2+TSX2(I),SOX3+TSX3(I))$$

CARD-H(I36);ITSH

ITSH : ITSH=-2 means end of CARD-G data.

If ISRC does not equal to 2, CARD-I, -J and -K are not necessary.

CARD-I(8E9.2);(SWX1(I),I=1,NSX1+1)

SWX1 : Weight of source strength for source location SOX1.

CARD-J(8E9.2);(SWX2(I),I=1,NSX2+1)

SWX2 : Weight of source strength for source location SOX2.

CARD-K(8E9.2);(SWX3(I),I=1,NSX3+1)

SWX3 : Weight of source strength for source location SOX3.

For combinatorial geometry input data, next CARD-CGA to CARD-CGE should be prepared.

CARD-CGA(2I5,10X,10A6);IVOPT,IDBG,JTY

IVOPT : Set to zero for PKN-HP input.

IDBG : Set to zero for PKN-HP input.

JTY : alphanumeric title for geometry input(columns 21-80)

CARD-CGB(2X,A3,1X,I4,6E10.3)

One set of CGB cards is required for each body and for the END card.(see Appendix A.16).

Leave columns 1-6 blank on all continuation cards.

ITYPE : specifies body type or END to terminate reading of body and (for example BOX, RPP, ARB, etc.). Leave blank for continuation cards.

IALP : body number assigned by user(all input body numbers must form a sequence set beginning at 1). If left blank, numbers are assigned sequentially. Either assign all or none of the numbers. Leave blank for continuation cards.

FPD(I) : real data required for the given body as shown in Appendix A.xx. This data must be in cm.

CARDS-CGC(2X,A3,I5,9(A2,I5))

Input zone specification cards. One set of cards required for each input zone, with input zone numbers being assigned sequentially.

IALP : IALP must be a nonblank for the first card of each set of cards defining an input zone. If IALP is blank, this card is treated as a continuation of the previous zone card. IALP = END denotes the end of zone description.

NAZ : total number of zones that can be entered upon leaving any of the bodies defined for this input region (some zones may be counted more than once). Leave blank for continuation cards for a given zone. (If NAZ < 0 on the first card of the zone card set, then it is set to 5). This is used to allocate blank common.

Alternate IIBIAS(I) and JTY(I) for all bodies defining this input zone.

IIBIAS(I): specify th "OR" operator if required for the JTY(I) body.

JTY(I) : body number with the (+) or (-) sign as required for the zone description.

CARDS-CGD(14I5)

MRIZ(I): MRIZ(I) is the region number in which the "Ith" input zone is contained (I=1, to the number of input zones). Region numbers must be sequentially defined from 1. Number 1 region should be a region including source.

CARDS-CGE(14I5)

MMIZ(I): MMIZ(I) is the medium number in which the "Ith" input zone is contained (I=1, to the number of input zones). Medium numbers must be sequentially defined from 1 to 3, else 0 for external void, or 1000 for internal void.

CARD-S(3I5,2E9.2); IPP,IPD(1),IPD(2),PD6A,PD6B

IPP : 0 (:ID number of energy dependence of neutron source.)
 (0,1-6)=(0:non neutron start;to be selected this in PKN-HP/1:mono energy n/2:spread energy n
 /3: ^{235}U fission n/4: ^{252}Cf fission n/5: $^{241}\text{Am-Be}$ n/6:spread energy n with Watt formula)

IPD(1) : 0 (:first group of input of source group information(-1~59))

IPD(2) : 0 (:last group of input of source group information(-1~59))

PD6A : 0 (: not need if IPP is not 6.)

PD6B : 0 (: not need if IPP is not 6.)

If IPP=6, neutron source strength is calculated according to the following equation,

$$S(E) \sim \exp(-PD6A \times E) \times \sinh(\sqrt{2} \times PD6B \times E),$$

where E is source neutron energy(MeV).

CARDS-T(8E9.3);(QID(I),I=1,IPD(2)-IPD(1)+1)

QID(I) : 0 (: The IPD(2)-IPD(1)+1 relative source strengths from IPD(1) to IPD(2) is necessary, if IPP=2. This card is not necessary when IPD(2) is larger than IPD(1). This card is ignored when IPP=6.)

CARDS-X(3E9.3,I9);(RX1(I),RX2(I),RX3(I),NGM(I),I=1,NDET(≤ 100))

RX1 : Calculational coordinates along X1-axis.

RX2 : Calculational coordinates along X2-axis.

RX3 : Calculational coordinates along X3-axis.

NGM : Coordinate system describing detector point

(0/1/2)=(Cylindrical/Cartesian/Spherical coordinate)

note: CARD-X is necessary to iterate by number of detector points, NDET.

CARD-Z(33x,i3);IZT

IZT = -1; The end of input data.

Appendix A.2 Input data of the Problem 1.

1	2	3	4	5	6	7	8	
PKN-HP-CG	SAMPLE PROBLEM 01					CARD PA		
500.	1.00E+06					CARD PB		
64.						CARD PC		
0.000	0.000	1.000				CARD PD		
PKN-H-CG	PROB. 01					CARD A		
2	2	2	3	3	0	1	2	CARD B
1.0	0.0		0.0		0.0		0.0	CARD C
0.0	2.5		5.0					CARD D
-5.	0.0		5.0					CARD E
0.0	180.		360.					CARD F
0.0	0.0		0.0		1.0			CARD G
						-2.		CARD H
1.0	1.0		1.0					CARD I
1.0	1.0		1.0					CARD J
1.0	1.0		1.0					CARD K
GEOMETRY DATA								CARDCGA
RCC	1	0.	0.	-2000.	0.	0.	4000.	CARDCGB
		575.						CARDCGB
RCC	2	0.	0.	-2000.	0.	0.	4000.	CARDCGB
		1475.						CARDCGB
RCC	3	0.	0.	-2000.	0.	0.	4000.	CARDCGB
		4000.						CARDCGB
END								CARDCGB
ZON		1						CARDCGC
ZON		-1	2					CARDCGC
ZON		-2	3					CARDCGC
END								CARDCGC
1	2	3						CARDCGD
1000	2	1000						CARDCGE
0	0	0						CARD S
0.00E+00								CARD T
0.00	0.	0.		0				CARD X
0.1	0.	0.		0				CARD X
10.	0.	0.		0				CARD X
40.	0.	0.		0				CARD X
100.	0.	0.		0				CARD X
200.	0.	0.		0				CARD X
300.	0.	0.		0				CARD X
400.	0.	0.		0				CARD X
574.5	0.	0.		0				CARD X
575.5	0.	0.		0				CARD X
580.	0.	0.		0				CARD X
577.	0.	0.		0				CARD X
600.	0.	0.		0				CARD X
700.	0.	0.		0				CARD X
825.	0.	0.		0				CARD X
900.	0.	0.		0				CARD X
1075.	0.	0.		0				CARD X
1200.	0.	0.		0				CARD X
1300.	0.	0.		0				CARD X

JAERI—Data/Code 96-020

1400.	0.	0.	0	CARD X
1475.	0.	0.	0	CARD X
1500.	0.	0.	0	CARD X
1600.	0.	0.	0	CARD X
1800.	0.	0.	0	CARD X
2000.	0.	0.	0	CARD X
			-1	CARD Z

Appendix A.3 Input data of the Problem 2.

1	2	3	4	5	6	7	8	
PKN-HP-CG PROBLEM 02							CARD PA	
1500. 1.00E+06							CARD PB	
238.							CARD PC	
0.000 0.000 1.000							CARD PD	
PKN-H-CG PROBLEM 02							CARD A	
2	10	2	6	6	0	1	2	CARD B
1.0		0.0		0.0		0.0		CARD C
0.0		2.5		5.0				CARD D
-75.		-60.		-45.		-30.		CARD E
45.		60.		75.				CARD F
0.0		180.		360.				CARD G
0.0		0.0		0.0		1.0		CARD H
						-2.		
1.0		1.0		1.0				CARD I
1.0		1.0		1.0		1.0		CARD J
1.0		1.0		1.0				CARD K
1.0		1.0		1.0				CARD K
GEOMETRY DATA								CARDCGA
RCC	1		0.		0.	-2000.		CARDCGB
			300.					CARDCGB
RCC	2		0.		0.	-2000.		CARDCGB
			1200.					CARDCGB
RCC	3		0.		0.	-2000.		CARDCGB
			4000.					CARDCGB
RPP	4		-300.		0.	-300.	300.	CARDCGB
RPP	5		-1200.		0.	-1200.	1200.	CARDCGB
RPP	6		-4000.		0.	-4000.	4000.	CARDCGB
END								CARDCGB
ZON			1					CARDCGC
ZON			4					CARDCGC
ZON			-1		-5	2		CARDCGC
ZON			-4		5			CARDCGC
ZON			-2		-5	3		CARDCGC
ZON			-5		6			CARDCGC
END								CARDCGC
1	2	3	4	5	6			CARDCGD
1000	1000	2	2	1000	1000			CARDCGE
0	0	0						CARD S
0.00E+00								CARD T
0.00		0.		0.		0		CARD X
0.1		0.		0.		0		CARD X
10.		0.		0.		0		CARD X
40.		0.		0.		0		CARD X
100.		0.		0.		0		CARD X
200.		0.		0.		0		CARD X
299.		0.		0.		0		CARD X
300.5		0.		0.		0		CARD X
310.		0.		0.		0		CARD X
350.		0.		0.		0		CARD X
450.		0.		0.		0		CARD X
550.		0.		0.		0		CARD X

JAERI-Data/Code 96-020

800.	0.	0.	0	CARD X
1050.	0.	0.	0	CARD X
1200.	0.	0.	0	CARD X
1500.	0.	0.	0	CARD X
2000.	0.	0.	0	CARD X
400.	-2000.	0.	0	CARD X
400.	-1500.	0.	0	CARD X
400.	-1000.	0.	0	CARD X
400.	-700.	0.	0	CARD X
400.	-500.	0.	0	CARD X
400.	-300.	0.	0	CARD X
400.	-200.	0.	0	CARD X
400.	-100.	0.	0	CARD X
400.	-75.	0.	0	CARD X
400.	-50.	0.	0	CARD X
400.	-25.	0.	0	CARD X
400.	0.	0.	0	CARD X
400.	25.	0.	0	CARD X
400.	50.	0.	0	CARD X
400.	75.	0.	0	CARD X
400.	100.	0.	0	CARD X
400.	200.	0.	0	CARD X
400.	300.	0.	0	CARD X
400.	500.	0.	0	CARD X
400.	700.	0.	0	CARD X
400.	1000.	0.	0	CARD X
400.	1500.	0.	0	CARD X
400.	2000.	0.	0	CARD X
			-1	CARD Z

Appendix A.5 Output of PKN-HP.

Calculational results are output corresponding to detector points describing in CARD-X. Neutron and secondary gamma-ray dose equivalents calculated with PKN-HP are listed, where the values of "finite thickness" represent the corrected one with finite medium effect³⁾.

Appendix A.6 Output data of the Problem 1.

ATTENUATION OF DOSE EQUIVALENT WITH PKN-HP INCIDENT PROTON ENERGY = 230. (MEV) < 64 CU-TARGET >				NEUTRON SOURCE POINTS = 8 Dose Equivalent			
NUM	X1	X2	X3	infinite thickness neutron [(μ Sv/hr)/(n/sec)]	2nd. γ	finite thickness neutron [(μ Sv/hr)/(n/sec)]	2nd. γ
1	0.00	0.00	0.00	2.714E-02	0.000E+00	2.714E-02	0.000E+00
2	0.10	0.00	0.00	2.711E-02	0.000E+00	2.711E-02	0.000E+00
3	10.00	0.00	0.00	2.701E-03	0.000E+00	2.701E-03	0.000E+00
4	40.00	0.00	0.00	1.928E-04	0.000E+00	1.928E-04	0.000E+00
5	100.00	0.00	0.00	3.110E-05	0.000E+00	3.110E-05	0.000E+00
6	200.00	0.00	0.00	7.785E-06	0.000E+00	7.785E-06	0.000E+00
7	300.00	0.00	0.00	3.461E-06	0.000E+00	3.461E-06	0.000E+00
8	400.00	0.00	0.00	1.947E-06	0.000E+00	1.947E-06	0.000E+00
9	574.50	0.00	0.00	9.438E-07	0.000E+00	9.438E-07	0.000E+00
10	575.50	0.00	0.00	4.126E-06	3.003E-08	4.126E-06	3.003E-08
11	580.00	0.00	0.00	3.025E-06	2.808E-08	3.025E-06	2.808E-08
12	577.00	0.00	0.00	3.718E-06	2.939E-08	3.718E-06	2.939E-08
13	600.00	0.00	0.00	8.192E-07	1.899E-08	8.192E-07	1.899E-08
14	700.00	0.00	0.00	1.227E-08	5.514E-10	1.227E-08	5.514E-10
15	825.00	0.00	0.00	3.233E-10	7.767E-12	3.233E-10	7.767E-12
16	900.00	0.00	0.00	4.092E-11	7.410E-13	4.092E-11	7.410E-13
17	1075.00	0.00	0.00	4.837E-13	8.676E-15	4.837E-13	8.676E-15
18	1200.00	0.00	0.00	2.538E-14	6.308E-16	2.538E-14	6.308E-16
19	1300.00	0.00	0.00	2.221E-15	5.050E-17	2.221E-15	5.050E-17
20	1400.00	0.00	0.00	2.027E-16	4.671E-18	2.027E-16	4.671E-18
21	1475.00	0.00	0.00	3.393E-17	7.929E-19	3.393E-17	7.929E-19
22	1500.00	0.00	0.00	3.280E-17	7.667E-19	2.167E-17	2.905E-19
23	1600.00	0.00	0.00	2.883E-17	6.739E-19	1.904E-17	2.553E-19
24	1800.00	0.00	0.00	2.278E-17	5.324E-19	1.505E-17	2.017E-19
25	2000.00	0.00	0.00	1.845E-17	4.313E-19	1.219E-17	1.634E-19

Appendix A.7 Output data of the Problem 2.

ATTENUATION OF DOSE EQUIVALENT WITH PKN-HP INCIDENT PROTON ENERGY = 1500 (MeV)				NEUTRON SOURCE POINTS=40			
< U-238-TARGET >				Dose equivalent			
NUM	X1	X2	X3	infinite thickness		finite thickness	
				neutron	2nd. γ ray [(μ Sv/hr)/(n/sec)]	neutron	2nd. γ ray [(μ Sv/hr)/(n/sec)]
1	0.00	0.00	0.00	1.373E-02	0.000E+00	1.373E-02	0.000E+00
2	0.10	0.00	0.00	1.373E-02	0.000E+00	1.373E-02	0.000E+00
3	10.00	0.00	0.00	6.434E-03	0.000E+00	6.434E-03	0.000E+00
4	40.00	0.00	0.00	1.288E-03	0.000E+00	1.288E-03	0.000E+00
5	100.00	0.00	0.00	3.044E-04	0.000E+00	3.044E-04	0.000E+00
6	200.00	0.00	0.00	8.453E-05	0.000E+00	8.453E-05	0.000E+00
7	299.00	0.00	0.00	3.869E-05	0.000E+00	3.869E-05	0.000E+00
8	300.50	0.00	0.00	1.827E-04	1.275E-06	1.827E-04	1.275E-06
9	310.00	0.00	0.00	8.738E-05	1.058E-06	8.738E-05	1.058E-06
10	350.00	0.00	0.00	5.067E-06	3.121E-07	5.067E-06	3.121E-07
11	450.00	0.00	0.00	1.414E-07	4.864E-09	1.414E-07	4.864E-09
12	550.00	0.00	0.00	1.168E-08	2.453E-10	1.168E-08	2.453E-10
13	800.00	0.00	0.00	3.182E-11	5.395E-13	3.182E-11	5.395E-13
14	1050.00	0.00	0.00	1.139E-13	2.498E-15	1.139E-13	2.498E-15
15	1200.00	0.00	0.00	3.735E-15	8.393E-17	3.735E-15	8.393E-17
16	1500.00	0.00	0.00	2.399E-15	5.391E-17	1.601E-15	1.933E-17
17	2000.00	0.00	0.00	1.353E-15	3.040E-17	9.029E-16	1.091E-17
18	400.00	-2000.00	0.00	8.846E-13	1.548E-14	8.846E-13	1.548E-14
19	400.00	-1500.00	0.00	1.952E-11	2.967E-13	1.952E-11	2.967E-13
20	400.00	-1000.00	0.00	5.775E-10	1.191E-11	5.775E-10	1.191E-11
21	400.00	-700.00	0.00	5.047E-09	1.466E-10	5.047E-09	1.466E-10
22	400.00	-500.00	0.00	2.250E-08	9.462E-10	2.250E-08	9.462E-10
23	400.00	-300.00	0.00	1.018E-07	6.482E-09	1.018E-07	6.482E-09
24	400.00	-200.00	0.00	2.067E-07	1.460E-08	2.067E-07	1.460E-08
25	400.00	-100.00	0.00	3.717E-07	2.609E-08	3.717E-07	2.609E-08
26	400.00	-75.00	0.00	4.181E-07	2.883E-08	4.181E-07	2.883E-08
27	400.00	-50.00	0.00	4.638E-07	3.123E-08	4.638E-07	3.123E-08
28	400.00	-25.00	0.00	5.069E-07	3.316E-08	5.069E-07	3.316E-08
29	400.00	0.00	0.00	5.457E-07	3.450E-08	5.457E-07	3.450E-08
30	400.00	25.00	0.00	5.786E-07	3.519E-08	5.786E-07	3.519E-08
31	400.00	50.00	0.00	6.046E-07	3.520E-08	6.046E-07	3.520E-08
32	400.00	75.00	0.00	6.231E-07	3.458E-08	6.231E-07	3.458E-08
33	400.00	100.00	0.00	6.333E-07	3.338E-08	6.333E-07	3.338E-08
34	400.00	200.00	0.00	6.009E-07	2.520E-08	6.009E-07	2.520E-08
35	400.00	300.00	0.00	4.958E-07	1.664E-08	4.958E-07	1.664E-08
36	400.00	500.00	0.00	2.692E-07	6.830E-09	2.692E-07	6.830E-09
37	400.00	700.00	0.00	1.197E-07	2.644E-09	1.197E-07	2.644E-09
38	400.00	1000.00	0.00	2.747E-08	4.929E-10	2.747E-08	4.929E-10
39	400.00	1500.00	0.00	1.889E-09	2.647E-11	1.889E-09	2.647E-11
40	400.00	2000.00	0.00	1.446E-10	2.375E-12	1.446E-10	2.375E-12

Appendix A.7 Output data of the Problem 2.

ATTENUATION OF DOSE EQUIVALENT WITH PKN-HP INCIDENT PROTON ENERGY = 1500 (MeV) < U-238-TARGET >				NEUTRON SOURCE POINTS=40 Dose equivalent			
NUM	X1	X2	X3	infinite thickness neutron [(μ Sv/hr)/(n/sec)]	2nd. γ ray	infinite thickness neutron [(μ Sv/hr)/(n/sec)]	2nd. γ ray
1	0.00	0.00	0.00	1.373E-02	0.000E+00	1.373E-02	0.000E+00
2	0.10	0.00	0.00	1.373E-02	0.000E+00	1.373E-02	0.000E+00
3	10.00	0.00	0.00	6.434E-03	0.000E+00	6.434E-03	0.000E+00
4	40.00	0.00	0.00	1.288E-03	0.000E+00	1.288E-03	0.000E+00
5	100.00	0.00	0.00	3.044E-04	0.000E+00	3.044E-04	0.000E+00
6	200.00	0.00	0.00	8.453E-05	0.000E+00	8.453E-05	0.000E+00
7	299.00	0.00	0.00	3.869E-05	0.000E+00	3.869E-05	0.000E+00
8	300.50	0.00	0.00	1.827E-04	1.275E-06	1.827E-04	1.275E-06
9	310.00	0.00	0.00	8.738E-05	1.058E-06	8.738E-05	1.058E-06
10	350.00	0.00	0.00	5.067E-06	3.121E-07	5.067E-06	3.121E-07
11	450.00	0.00	0.00	1.414E-07	4.864E-09	1.414E-07	4.864E-09
12	550.00	0.00	0.00	1.168E-08	2.453E-10	1.168E-08	2.453E-10
13	800.00	0.00	0.00	3.182E-11	5.395E-13	3.182E-11	5.395E-13
14	1050.00	0.00	0.00	1.139E-13	2.498E-15	1.139E-13	2.498E-15
15	1200.00	0.00	0.00	3.735E-15	8.393E-17	3.735E-15	8.393E-17
16	1500.00	0.00	0.00	2.399E-15	5.391E-17	1.601E-15	1.933E-17
17	2000.00	0.00	0.00	1.353E-15	3.040E-17	9.029E-16	1.091E-17
18	400.00	-2000.00	0.00	8.846E-13	1.548E-14	8.846E-13	1.548E-14
19	400.00	-1500.00	0.00	1.952E-11	2.967E-13	1.952E-11	2.967E-13
20	400.00	-1000.00	0.00	5.775E-10	1.191E-11	5.775E-10	1.191E-11
21	400.00	-700.00	0.00	5.047E-09	1.466E-10	5.047E-09	1.466E-10
22	400.00	-500.00	0.00	2.250E-08	9.462E-10	2.250E-08	9.462E-10
23	400.00	-300.00	0.00	1.018E-07	6.482E-09	1.018E-07	6.482E-09
24	400.00	-200.00	0.00	2.067E-07	1.460E-08	2.067E-07	1.460E-08
25	400.00	-100.00	0.00	3.717E-07	2.609E-08	3.717E-07	2.609E-08
26	400.00	-75.00	0.00	4.181E-07	2.883E-08	4.181E-07	2.883E-08
27	400.00	-50.00	0.00	4.638E-07	3.123E-08	4.638E-07	3.123E-08
28	400.00	-25.00	0.00	5.069E-07	3.316E-08	5.069E-07	3.316E-08
29	400.00	0.00	0.00	5.457E-07	3.450E-08	5.457E-07	3.450E-08
30	400.00	25.00	0.00	5.786E-07	3.519E-08	5.786E-07	3.519E-08
31	400.00	50.00	0.00	6.046E-07	3.520E-08	6.046E-07	3.520E-08
32	400.00	75.00	0.00	6.231E-07	3.458E-08	6.231E-07	3.458E-08
33	400.00	100.00	0.00	6.333E-07	3.338E-08	6.333E-07	3.338E-08
34	400.00	200.00	0.00	6.009E-07	2.520E-08	6.009E-07	2.520E-08
35	400.00	300.00	0.00	4.958E-07	1.664E-08	4.958E-07	1.664E-08
36	400.00	500.00	0.00	2.692E-07	6.830E-09	2.692E-07	6.830E-09
37	400.00	700.00	0.00	1.197E-07	2.644E-09	1.197E-07	2.644E-09
38	400.00	1000.00	0.00	2.747E-08	4.929E-10	2.747E-08	4.929E-10
39	400.00	1500.00	0.00	1.889E-09	2.647E-11	1.889E-09	2.647E-11
40	400.00	2000.00	0.00	1.446E-10	2.375E-12	1.446E-10	2.375E-12

Appendix A.8 Output data of the Problem 3.

ATTENUATION OF DOSE EQUIVALENT WITH PKN-HP INCIDENT PROTON ENERGY = 230 (MeV) < 64 CU-TARGET >				NEUTRON SOURCE POINTS = 8 Dose equivalent			
NUM	X1	X2	X3	infinite thickness		finite thickness	
				neutron [(μ Sv/hr)/(n/sec)]	2nd. γ ray [(μ Sv/hr)/(n/sec)]	neutron [(μ Sv/hr)/(n/sec)]	2nd. γ ray [(μ Sv/hr)/(n/sec)]
1	0.00	0.00	0.00	6.114E-03	0.000E+00	6.114E-03	0.000E+00
2	1.00	0.00	0.00	6.395E-03	0.000E+00	6.395E-03	0.000E+00
3	5.00	0.00	0.00	4.351E-03	0.000E+00	4.351E-03	0.000E+00
4	10.00	0.00	0.00	1.645E-03	0.000E+00	1.645E-03	0.000E+00
5	30.00	0.00	0.00	2.221E-04	0.000E+00	2.221E-04	0.000E+00
6	49.90	0.00	0.00	8.154E-05	0.000E+00	8.154E-05	0.000E+00
7	50.10	0.00	0.00	2.731E-04	1.877E-06	2.731E-04	1.877E-06
8	52.00	0.00	0.00	2.332E-04	1.730E-06	2.332E-04	1.730E-06
9	55.00	0.00	0.00	1.836E-04	1.527E-06	1.836E-04	1.527E-06
10	65.00	0.00	0.00	9.011E-05	1.032E-06	9.011E-05	1.032E-06
11	100.00	0.00	0.00	1.516E-05	3.020E-07	1.516E-05	3.020E-07
12	150.00	0.00	0.00	2.584E-06	6.458E-08	2.584E-06	6.458E-08
13	200.00	0.00	0.00	5.564E-07	1.472E-08	5.564E-07	1.472E-08
14	250.00	0.00	0.00	1.284E-07	3.149E-09	1.284E-07	3.149E-09
15	300.00	0.00	0.00	3.068E-08	6.479E-10	3.068E-08	6.479E-10
16	350.00	0.00	0.00	7.571E-09	1.362E-10	7.571E-09	1.362E-10
17	450.00	0.00	0.00	5.175E-10	7.854E-12	5.175E-10	7.854E-12
18	550.00	0.00	0.00	3.464E-10	5.258E-12	2.276E-10	2.051E-12
19	750.00	0.00	0.00	1.863E-10	2.828E-12	1.224E-10	1.103E-12
20	0.00	22.00	0.00	4.041E-04	0.000E+00	4.041E-04	0.000E+00
21	1.00	22.00	0.00	6.184E-03	0.000E+00	6.184E-03	0.000E+00
22	5.00	22.00	0.00	3.570E-03	0.000E+00	3.570E-03	0.000E+00
23	10.00	22.00	0.00	1.378E-03	0.000E+00	1.378E-03	0.000E+00
24	30.00	22.00	0.00	1.861E-04	0.000E+00	1.861E-04	0.000E+00
25	49.90	22.00	0.00	6.838E-05	0.000E+00	6.838E-05	0.000E+00
26	50.10	22.00	0.00	2.397E-04	1.676E-06	2.397E-04	1.676E-06
27	52.00	22.00	0.00	2.031E-04	1.541E-06	2.031E-04	1.541E-06
28	55.00	22.00	0.00	1.580E-04	1.354E-06	1.580E-04	1.354E-06
29	65.00	22.00	0.00	7.437E-05	9.002E-07	7.437E-05	9.002E-07
30	100.00	22.00	0.00	1.112E-05	2.435E-07	1.112E-05	2.435E-07
31	150.00	22.00	0.00	1.737E-06	4.605E-08	1.737E-06	4.605E-08
32	200.00	22.00	0.00	3.543E-07	9.708E-09	3.543E-07	9.708E-09
33	250.00	22.00	0.00	7.827E-08	1.969E-09	7.827E-08	1.969E-09
34	300.00	22.00	0.00	1.803E-08	3.882E-10	1.803E-08	3.882E-10
35	350.00	22.00	0.00	4.305E-09	7.872E-11	4.305E-09	7.872E-11
36	450.00	22.00	0.00	2.779E-10	4.267E-12	2.779E-10	4.267E-12
37	550.00	22.00	0.00	1.861E-10	2.857E-12	1.220E-10	1.126E-12
38	750.00	22.00	0.00	1.001E-10	1.537E-12	6.562E-11	6.054E-13
39	0.00	45.00	0.00	1.001E-04	0.000E+00	1.001E-04	0.000E+00
40	1.00	45.00	0.00	5.728E-03	0.000E+00	5.728E-03	0.000E+00
41	5.00	45.00	0.00	2.510E-03	0.000E+00	2.510E-03	0.000E+00
42	10.00	45.00	0.00	9.488E-04	0.000E+00	9.488E-04	0.000E+00

43	30.00	45.00	0.00	1.260E-04	0.000E+00	1.260E-04	0.000E+00
44	49.90	45.00	0.00	4.624E-05	0.000E+00	4.624E-05	0.000E+00
45	50.10	45.00	0.00	1.800E-04	1.293E-06	1.800E-04	1.293E-06
46	52.00	45.00	0.00	1.499E-04	1.182E-06	1.499E-04	1.182E-06
47	55.00	45.00	0.00	1.134E-04	1.030E-06	1.134E-04	1.030E-06
48	65.00	45.00	0.00	4.817E-05	6.625E-07	4.817E-05	6.625E-07
49	100.00	45.00	0.00	5.035E-06	1.484E-07	5.035E-06	1.484E-07
50	150.00	45.00	0.00	5.776E-07	1.920E-08	5.776E-07	1.920E-08
51	200.00	45.00	0.00	9.653E-08	3.035E-09	9.653E-08	3.035E-09
52	250.00	45.00	0.00	1.813E-08	5.023E-10	1.813E-08	5.023E-10
53	300.00	45.00	0.00	3.621E-09	8.414E-11	3.621E-09	8.414E-11
54	350.00	45.00	0.00	7.599E-10	1.481E-11	7.599E-10	1.481E-11
55	450.00	45.00	0.00	3.888E-11	6.291E-13	3.888E-11	6.291E-13
56	550.00	45.00	0.00	2.603E-11	4.211E-13	1.695E-11	1.719E-13
57	750.00	45.00	0.00	1.400E-11	2.265E-13	9.118E-12	9.244E-14
58	0.00	90.00	0.00	2.332E-05	4.230E-07	2.332E-05	4.230E-07
59	1.00	90.00	0.00	5.213E-03	0.000E+00	5.213E-03	0.000E+00
60	5.00	90.00	0.00	1.543E-03	0.000E+00	1.543E-03	0.000E+00
61	10.00	90.00	0.00	5.335E-04	0.000E+00	5.335E-04	0.000E+00
62	49.90	90.00	0.00	2.475E-05	0.000E+00	2.475E-05	0.000E+00
63	50.10	90.00	0.00	1.121E-04	7.985E-07	1.121E-04	7.985E-07
64	52.00	90.00	0.00	9.112E-05	7.273E-07	9.112E-05	7.273E-07
65	55.00	90.00	0.00	6.612E-05	6.292E-07	6.612E-05	6.292E-07
66	65.00	90.00	0.00	2.390E-05	3.934E-07	2.390E-05	3.934E-07
67	100.00	90.00	0.00	1.129E-06	7.004E-08	1.129E-06	7.004E-08
68	150.00	90.00	0.00	4.513E-08	4.170E-09	4.513E-08	4.170E-09
69	200.00	90.00	0.00	4.008E-09	2.581E-10	4.008E-09	2.581E-10
70	250.00	90.00	0.00	4.979E-10	2.056E-11	4.979E-10	2.056E-11
71	300.00	90.00	0.00	7.448E-11	2.141E-12	7.448E-11	2.141E-12
72	350.00	90.00	0.00	1.275E-11	2.798E-13	1.275E-11	2.798E-13
73	450.00	90.00	0.00	5.085E-13	8.606E-15	5.085E-13	8.606E-15
74	550.00	90.00	0.00	3.404E-13	5.760E-15	2.199E-13	2.475E-15
75	750.00	90.00	0.00	1.830E-13	3.098E-15	1.182E-13	1.331E-15

Appendix A.9 Input Required on CGB Cards for Each Body Type*

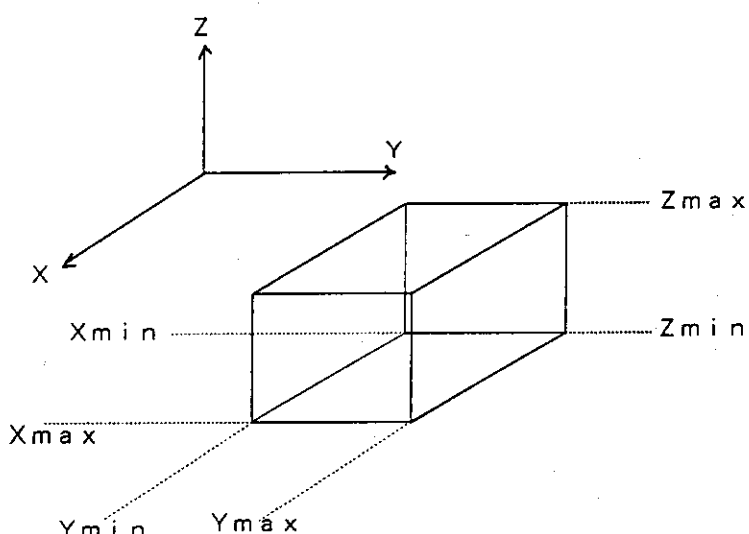
Card Columns Body Type	ITYPE A3	IALP 3-5	Real Data Defining Particular Body 11-20 21-30 31-40 41-50 51-60 61-70	Number of Cards Needed
Box	BOX	ILAP is assigned by the user or by the	Vx Vy Vz H1x H1y H1z H2x H2y H2z H3x H3y H3z	1 of 2 2 of 2
Right Parallel piped	RPP	Right Circular Cylinder	Xmin Xmax Ymin Ymax Zmin Zmax	1
Sphere	SPH	code if left	Vx Vy Vz R	- - - 1
Elliptic Cylinder	RCC	blank.	Vx Vy Vz Hx Hy Hz R	1 of 2 2 of 2
Ellipsoid	REC	Vx R1x Vy R1y Vz R1z	Hx R2x Hy R2y Hz R2z	1 of 2 2 of 2
Truncated Right Cone	ELL	V1x V1y V1z	V2x V2y V2z	1 of 2 2 of 2
Right Angle Wedge	TRC	Vx Vy Vz Hx Hy Hz L1 L2	- - - - - -	1 of 2 2 of 2
Arbitrary Polyhedron	WED or RAW	Vx H2x Vy H2y Vz H2z H1x H1y H1z H3x H3y H3z	- - - - - -	1 of 2 2 of 2
	ARB	V1x V1y V1z V2x V2y V2z V3x V3y V3z V4x V4y V4z V5x V5y V5z V6x V6y V6z V7x V7y V7z V8x V8y V8z	- - - - - -	1 of 5 2 of 5 3 of 5 4 of 5
			Face Descriptions (see note below)	5 of 5
Termination of Body Input Data	END			

*) from M.B. Emmett: "The MORSE Monte Carlo Radiation Transport Code System", ORNL-4972(1975), 4.3-9 to 4.3-10.

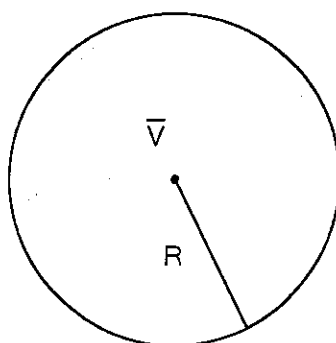
Note: Card 5 of the arbitrary polyhedron input contains a four-digit number for each of the six faces of an ARB body. The format is 6D10.3, beginning in column 11. See the ARB write-up section 4.7 in reference *) for an example.

Appendix A.10 Description of Body Types*

The information required to specify each type of body is as follows:

a. Rectangular Parallelepiped (RPP)

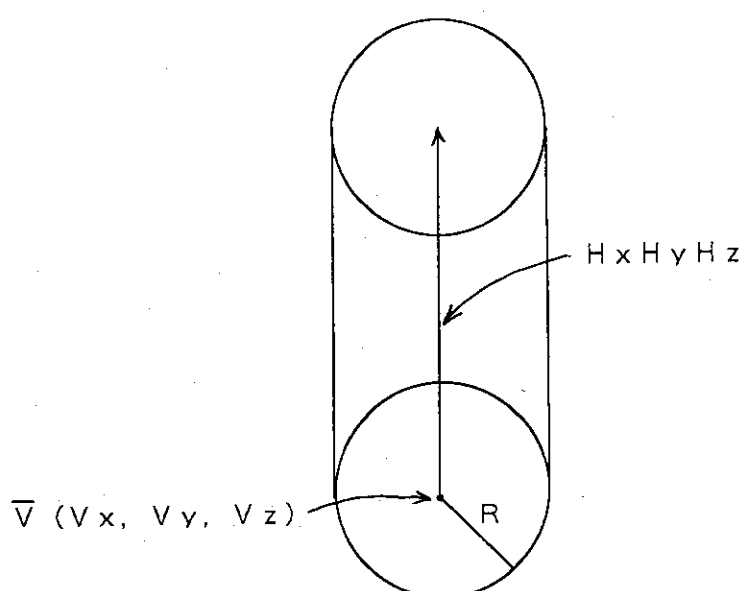
X_{\max} : the maximum value
 of x coordinates
 X_{\min} : the minimum value
 of x coordinates
 Y_{\max} : the maximum value
 of y coordinates
 Y_{\min} : the minimum value
 of y coordinates
 Z_{\max} : the maximum value
 of z coordinates
 Z_{\min} : the minimum value
 of z coordinates

b. Sphere (SPH)

R : radius
 \bar{V} : the vertex at the
 center.

*) from M. B. Emmett:"The MORSE Monte Carlo Radiation Transport Code System". ORNL-4972(1975), 4.7.3.

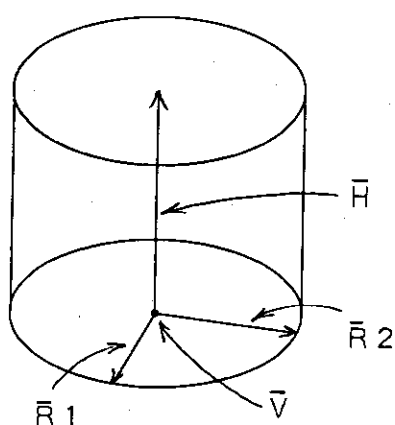
c. Right Circular Cylinder (RCC)



\bar{V} : the vertex at the center of one base.
 \bar{H} : a height vector

R : radius

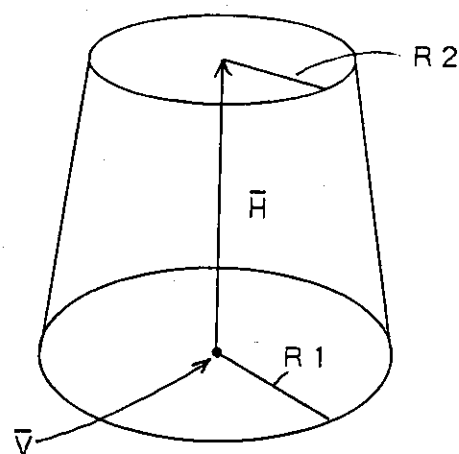
d. Right Elliptical Cylinder (REC)



\bar{V} : the vertex at the center of one base.
 \bar{H} : a height vector

\bar{R}_1, \bar{R}_2 :
a vector in the plane of the base defining the major and minor axes.

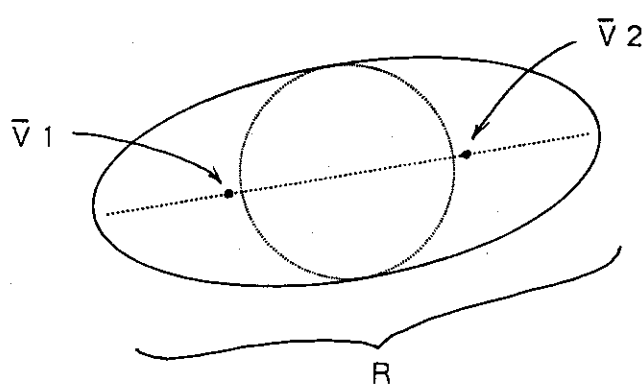
e. Truncated Right Angle Cone (TRC)



\bar{V} : the vertex at the center of one base.
 \bar{H} : a height vector

R_1, R_2 : the radii of the lower and upper bases.

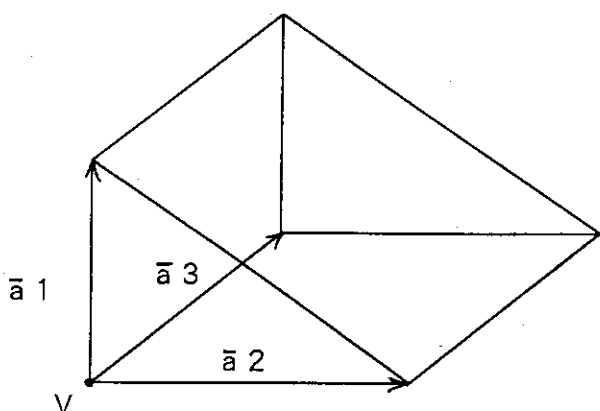
f. Ellipsoid (ELL)



V_1, V_2 :
two vertices denoting the coordinates of the foci.

R : the length of the major axis.

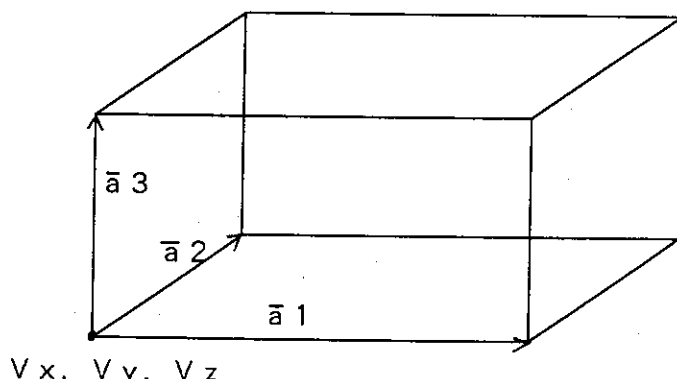
g. Wedge (WED) or (RAW)



\bar{v} : the vertex at one of the corners.

$\bar{a}_1, \bar{a}_2, \bar{a}_3$: a set of three mutually perpendicular vectors.

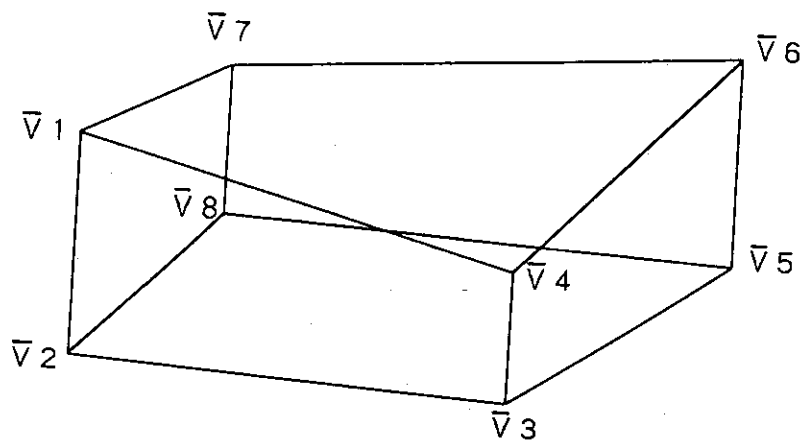
h. Box (BOX)



\bar{v} : the vertex at one of the corners.

$\bar{a}_1, \bar{a}_2, \bar{a}_3$: a set of three mutually perpendicular vectors.

i. Arbitrary Polyhedron (ARB)



$\bar{V}_1, \bar{V}_2, \bar{V}_3, \bar{V}_4, \bar{V}_5, \bar{V}_6,$
 $\bar{V}_7, \bar{V}_8 :$

eight vertices,
must be entered in
either clockwise or
counterclockwise
order.

Appendix A.11 Calculation conditions of neutron and secondary gamma-ray dose equivalent attenuation data installed in PKN-HP.

Code	ANISN-JR ¹⁾ : 1-dimensional discrete ordinates transport calculation code		
Cross section library	HILO86R ²⁾ : (P_5) effective macroscopic cross section		
Number of energy group	neutron 66 groups (from thermal to 400 MeV) gamma-ray 22 groups (from 0.01 to 20 MeV)		
Source	point isotropic 55 monoenergetic neutrons (from 0.01 to 400 MeV)		
Shielding material	water, ordinary concrete and iron		
Geometry	1-dimensional sphere (S_{16})		
Flux to dose equivalent conversion factors	neutron	$E > 20$ MeV	Maximum dose ^{*)}
		$E \leq 20$ MeV	1 cm depth dose ^{**)}
	gamma-ray	$E > 10$ MeV	Maximum dose ^{*)}
		$E \leq 10$ MeV	1 cm depth dose ⁺⁺⁾

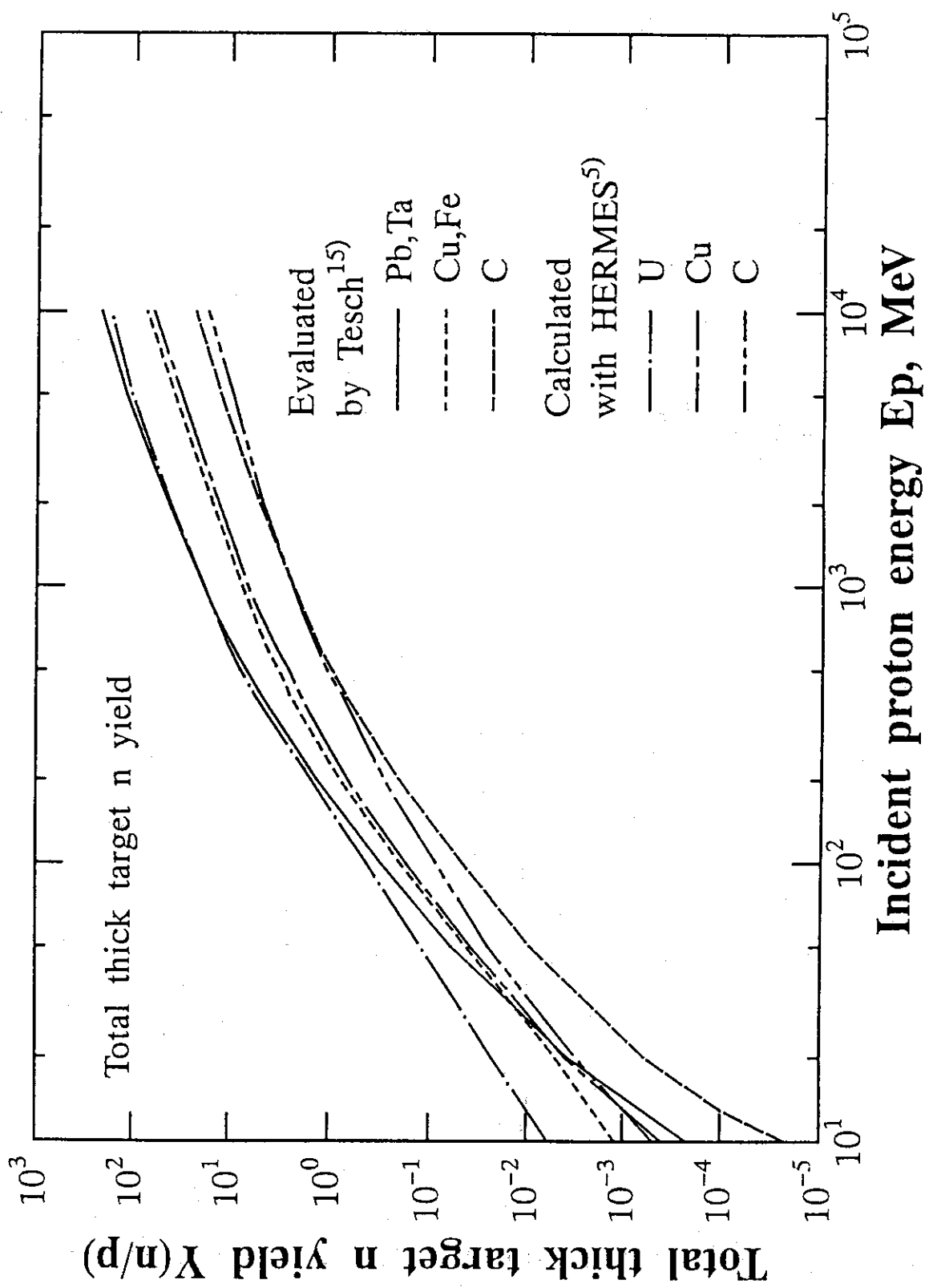
*) ICRP Publication 51(1987),p.39,Table 23.

**) ibid.,p.36,Table 21.

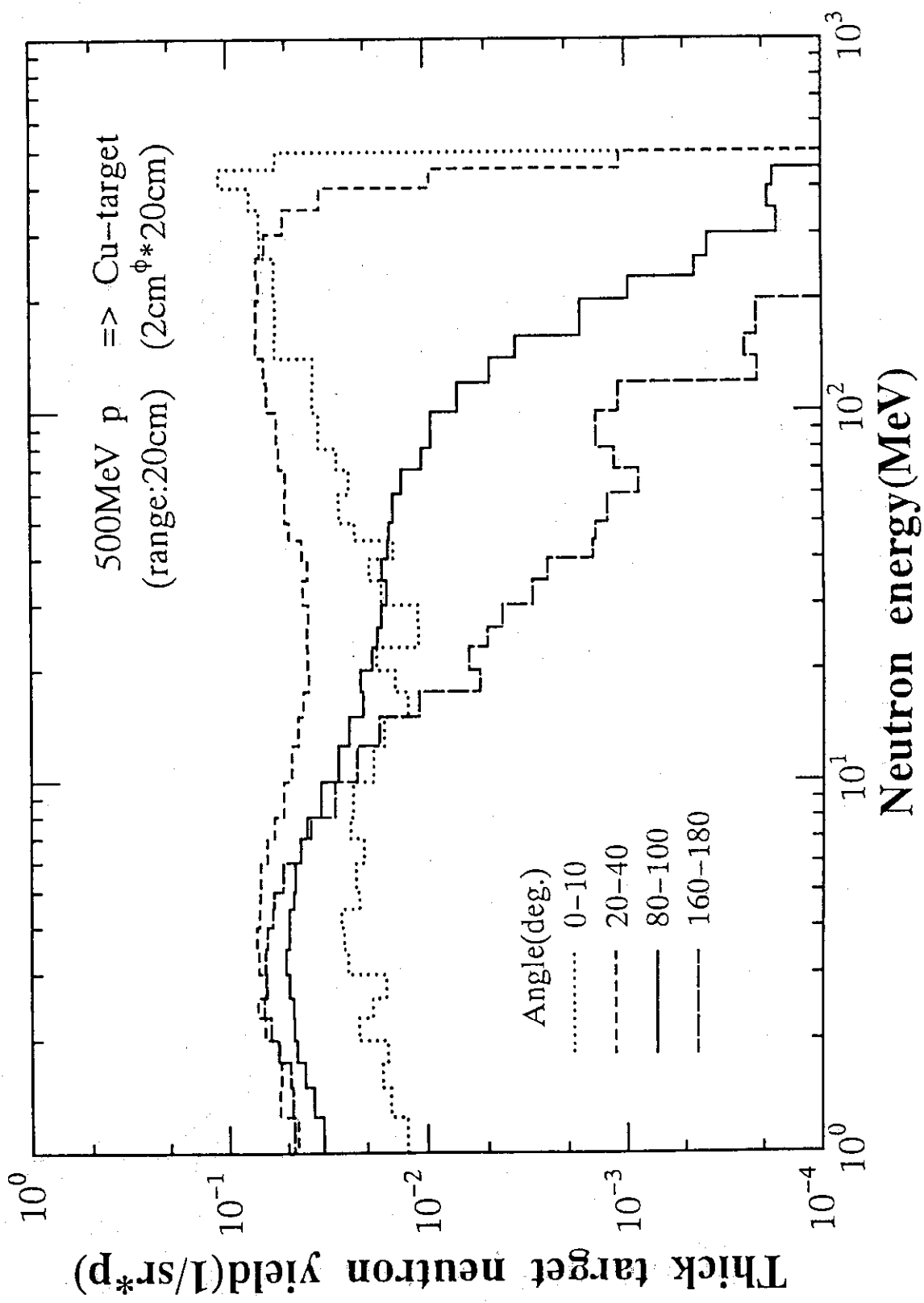
+) ibid.,p.26,Table 14.

++) ibid.,p.22,Table 10.

Appendix A.12 Comparisons of total thick target neutron yields between various target materials and between two evaluation methods



Appendix A.13 Double differential thick target neutron yield calculated with HETC for 500 MeV proton bombardment on full stopping length Cu target



Appendix A.14: Double differential thick target neutron yield calculated with HETC for 2 GeV proton bombardment on full stopping length U-238 target

